DEVELOPMENT OF A PARTICLE BREAKAGE MODEL FOR IMPLEMENTATION IN THE DISCRETE ELEMENT METHOD

Anderson Silva das Chagas

Dissertação de Mestrado apresentada ao Programa de Pós-graduação em Engenharia Metalúrgica e de Materiais, COPPE, da Universidade Federal do Rio de Janeiro, como parte dos requisitos necessários à obtenção do título de Mestre em Engenharia Metalúrgica e de Materiais.

Orientador: Luís Marcelo Marques Tavares

Rio de Janeiro
Dezembro de 2019

DEVELOPMENT OF A PARTICLE BREAKAGE MODEL FOR IMPLEMENTATION IN THE DISCRETE ELEMENT METHOD

Anderson Silva das Chagas

DISSERTAÇÃO SUBMETIDA AO CORPO DOCENTE DO INSTITUTO ALBERTO LUIZ COIMBRA DE PÓS-GRADUAÇÃO E PESQUISA DE ENGENHARIA (COPPE) DA UNIVERSIDADE FEDERAL DO RIO DE JANEIRO COMO PARTE DOS REQUISITOS NECESSÁRIOS PARA A OBTENÇÃO DO GRAU DE MESTRE EM CIÊNCIAS EM ENGENHARIA METALÚRGICA E DE MATERIAIS.

Orientador: Prof. Luís Marcelo Marques Tavares, Ph.D

Aprovada por: Prof. Rodrigo Magalhães de Carvalho, D.Sc.
Prof. José Luis Drummond Alves, D.Sc.

RIO DE JANEIRO, RJ – BRASIL
DEZEMBRO DE 2019

das Chagas, Anderson Silva

Development of a particle breakage model for implementation in the discrete element method/ Anderson Silva das Chagas. – Rio de Janeiro: UFRJ/COPPE, 2019.

XV, 127 p.: il.; 29,7 cm.

Orientador: Luís Marcelo Marques Tavares

Dissertação (mestrado) – UFRJ/ COPPE/ Programa de Engenharia Metalúrgica e Materiais, 2019.

Referências Bibliográficas: p. 120-127.

1. Cominuição. 2. Método dos elementos discretos. 3. EDEM. I. Tavares, Luís Marcelo Marques. II. Universidade Federal do Rio de Janeiro, COPPE, Programa de Engenharia Metalúrgica e de Materiais. III. Título.

Resumo da Dissertação apresentada à COPPE/UFRJ como parte dos requisitos necessários para a obtenção do grau de Mestre em Ciências (M.Sc.)

DEVELOPMENT OF A PARTICLE BREAKAGE MODEL FOR IMPLEMENTATION IN THE DISCRETE ELEMENT METHOD

Anderson Silva das Chagas

Dezembro/2019

Orientador: Luís Marcelo Marques Tavares

Programa: Engenharia Metalúrgica e de Materiais

Quebra de partículas no Método de Elementos Discretos (DEM) é imprescindível na simulação de várias operações, como é o caso da britagem. Assim, o presente trabalho tem por objetivo desenvolver um modelo de quebra de partículas em DEM, baseado no modelo de substituição de partículas. Para descrever apropriadamente a fragmentação mineral, serão acoplados microprocessos relacionados à quebra ao algoritmo de simulação. Tanto as propriedades de quebra das partículas quanto o tamanho dos fragmentos gerados seguem distribuições estatísticas verificadas em materiais frágeis, conferindo variabilidade ao produto. A implementação do modelo foi realizada através de uma API para acoplamento no software comercial EDEM. Para validação do modelo, foram comparados resultados da simulação a dados de ensaios de queda de peso livre em partículas e quebra autógena de partículas por queda livre, mostrando boa correspondência.

Abstract of the Dissertation presented to COPPE/UFRJ as part of the necessary requirements to obtain the title of Master of Science (M.Sc.)

DEVELOPMENT OF A PARTICLE BREAKAGE MODEL FOR IMPLEMENTATION IN THE DISCRETE ELEMENT METHOD

Anderson Silva das Chagas

December/2019

Advisor: Prof. Luís Marcelo Marques Tavares

Program: Metallurgical and Materials Engineering

Particle breakage in the Discrete Element Method (DEM) is indispensable in the simulation of various unit operations, which is the case of crushing. Thus, the present work aims to develop a particle breakage model in DEM, based on the particle replacement model. In order to properly describe particle fragmentation, microprocesses related to breakage are coupled to the simulation algorithm. Both particle breakage properties and size of the generated fragments follow statistical distributions that have previously demonstrated to be valid for brittle materials, being able to describe the variability observed in practice. The implementation of the model has been carried out through an API for coupling in the commercial software EDEM. In order to validate the model, data from drop weight tests on particles as well as drop tests are compared to simulations, demonstrating good agreement.

SUMÁRIO

I. INTRODUCTION

Granular materials are extremely important in many industrial processes, including in science and in everyday life. Unlike other materials, handling of granular materials is often extremely challenging, as they exhibit very different behavior under various circumstances. A fluidized granular bed often behaves like a liquid: it flows through pipes, presents wave formation, flows in an hourglass, etc. In other situations, its behavior resembles a solid: a pile of sand does not dissolve by itself, but can be plastically deformed. When the grains are coarse enough (d>250 μm) and the surrounding fluid is not very viscous, the mechanical properties of the material are controlled only by moment transfer during collision or friction between grains (Brown & Richards 1970). However, the flow of dry granular materials is not easily described.

In several industries, particularly in the minerals industry, understanding and describing the behavior of granular materials becomes even more complex, since breakage of particles can occur and should be considered. In industrial equipment, such as crushers and mills, particles break, generating not only a family of smaller particles, contained in several sizes, but also with shapes of the most varied types. It is noted that the complete description, both of the behavior of the granular load, and of the product and energy input in equipment and processes in general, is extremely complex, despite its importance.

Comminution equipment are generally described as machines that handle the material and that are capable of applying energy to fracture it. This particulate material is fractured as a result of the application of tensile, compressive and shear forces. Despite having been developed for a high level of mechanical efficiency and robustness, operation of comminution equipment is costly in terms of energy consumed. In a typical mineral processing plant, about 35% to 50% of the operating cost is related to comminution (Curry et al. 2014). Thus, the importance of understanding the flow and fragmentation of particulate material in these processes becomes clear.

The Discrete Element Method (DEM) is a powerful tool for analysis of the internal dynamics of equipment and systems. DEM is a computational method that allows the prediction of particle flow, allowing the description of the behavior both in the individual particle scale, as well as in the process as a whole. In DEM, the movement of each individual particle is calculated by applying Newton's laws while their interactions are simulated using a set of equations, referred to as contact model (Weerasekara et al. 2013). The contact model determines the forces and dissipated energies associated with the interactions between particles, as well as interactions with the geometry of the devices.

DEM alone is not able to predict breakage in the granular material. Traditionally and whenever pertinent, the particle flow and the energy spectrum involved in the collisions have been extracted from the simulations and applied to support methodologies in order to predict breakage at a post-processing stage. This has been applied successfully to mills and some types of crushers (Powell et al. 2008; Tavares & Carvalho 2009).

In recent years, auxiliary algorithms have been proposed in order to simulate fragmentation of particles in DEM environment. These are the models of tetrahedral elements (Potapov & Campbell 1994), connected spheres (Potyondy & Cundall 2004) and particle replacement (Cleary 2001). Thus, DEM with appropriate description of particle breakage is presented with a complete solution and free of empiricism in the description of comminution processes, since it directly simulates not only motion of the material but also the product of the process.

However, some of the alternatives currently available for simulation of breakage in DEM environment are too simplistic in the description of the complexity found in fragmentation of mineral particles. The present work proposes to develop a dynamic particle breakage model, with a framework based on the existing approaches, for implementation in DEM simulations in the commercial software EDEM. Models of ore fragmentation micro-processes that have been the result of research group at the Laboratório de Tecnologia Mineral from COPPE/UFRJ are adapted and implemented in the DEM environment.

II. REVIEW OF THE LITERATURE

II.1.1 Particle breakage

Particle fragmentation represents the most elementary process in comminution of ores. Thus, the study of the phenomena involved in fracture of individual particles constitutes a basis for the assessment of the energy consumption in the reduction of particles in size in comminution processes.

Even the results of a single particle breakage event are not fully predictable due to the large number of variables that affect the result. Therefore, studies trying to understand this process have directed their attention to breakage of individual particles under specific sets of conditions. These studies focus on particle strength, the energy consumed in a fragmentation event, and the size distribution of the fragments produced in that event. The behavior observed in the laboratory often gives important clues about the complex behavior of commercial comminution equipment.

In industrial equipment, particles are generally fragmented as a result of single impact, double impact and slow compression loads, which are illustrated in Figure II.1. Thus, individual particle fragmentation studies have been conducted since the 1960s in order to elucidate phenomena such as (Tavares 2007):

- energy consumed in comminution;
- particle size effect, shape, composition, loading mode;
- relationship between energy and size reduction;
- degradation processes;
- deformation of the material under loading.

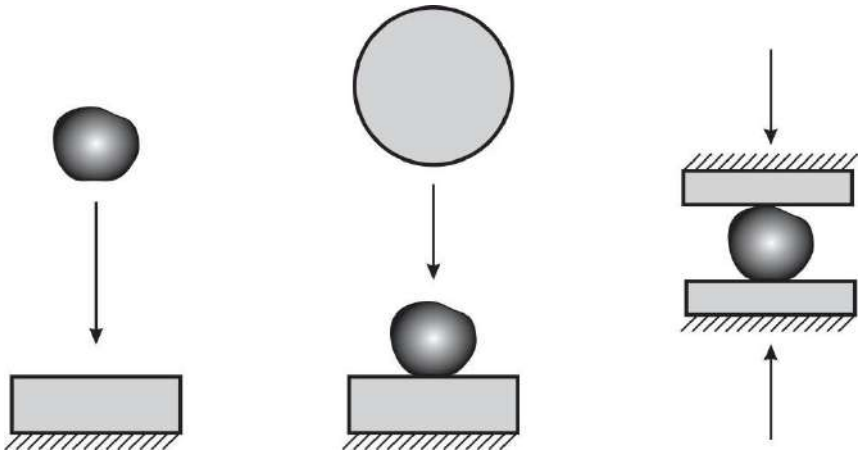

Figure II.1 – Typical modes of application of stresses in industrial equipment.

Currently the mechanisms involved in mineral particle breakage are fairly very well described and understood, so that there is some consensus in the literature regarding its basic description (Tavares 2007). From the initial moment of contact with a surface, as in the cases mentioned above, the particle suffers a stress and energy is accumulated in the form of deformation. Due to the typically brittle nature of mineral particles, plastic deformation is generally disregarded. In addition to some deformation, damage in the form of small cracks begin to accumulate inside the particle and when a breakage criterion is reached, a macrocrack grows unstably causing the volumetric fragmentation of the particle (Tavares & King 1998). The size distribution of the generated fragments depends on the size and location of the initial crack, the microstructure of the original particle and the amenability of a crack to branch during its propagation inside the particle.

The fracture process of the particle does not end after the initial fracture since there may still be kinetic energy from the apparatus exerting force on the previously generated fragments. This remaining energy must be dissipated in the following instants, which can result in fragment projection, secondary breakage of the initial fragment, and consecutive breakage stages.

II.1.2 Breakage characteristics

II.1.2.1 Fracture energy and probability of fracture distribution

Fragmentation of particulate matter is a random process. Many factors, such as shape, size, surface area, mineralogical composition and internal structure, contribute to the fracture of individual particles and the result is never fully predictable (King 2001).

Although there is no certainty about the fragmentation of a particular particle involved in an impact, it is possible to relate the probability of fracture to the amount of energy that is absorbed by the particle during the impact. When a particle is subjected to loading it is able to absorb only a certain amount of energy before fracturing. This amount is called the fracture energy of the particle and is an individual property of the particle (Tavares 2007). Particles of the same material, similar shape and size, present a wide variety of individual fracture energies. This fact reflects the random nature of the fracture process and the large distribution of existing microscopic flaws in naturally formed particle populations.

The fracture probability distribution of a sample describes the probability that a particle, of a given material and size, will fragment as a result of application of a load as a function

of the applied energy. In this context, irregularly shaped particles that have lost at least 10% of their original mass in a charge are considered broken (Tavares 2007). Fracture probability is determined by individually loading a large enough number of particles (typically 100 particles), of a given material and size, with fixed loading intensity and verifying the proportion of particles being broken as a function of the applied energy.

Fracture energy or fracture probability data can be described using an appropriate statistical distribution. Lognormal and truncated lognormal distributions have been the most commonly adopted in describing fracture energy data for a variety of irregularly shaped brittle materials (Baumgardt et al. 1975; King & Bourgeois 1993; Tavares & King 1998). Figure II.2 shows the distribution of fracture energies for quartz particles in different size ranges, and the lines represent the fit to the lognormal distribution. Note that the particle size affects the energy required to break this material, with finer particles presenting higher fracture energies. The lognormal distribution can be written as

$$F(E_f) = \frac{1}{2}\left[1 + erf\left(\frac{\ln E_f - \ln E_{f50}}{\sqrt{2}\sigma_E}\right)\right] \qquad \text{II.1}$$

in which E_{f50} and σ_E are the median energy of fracture and the standard deviation of the distribution, respectively.

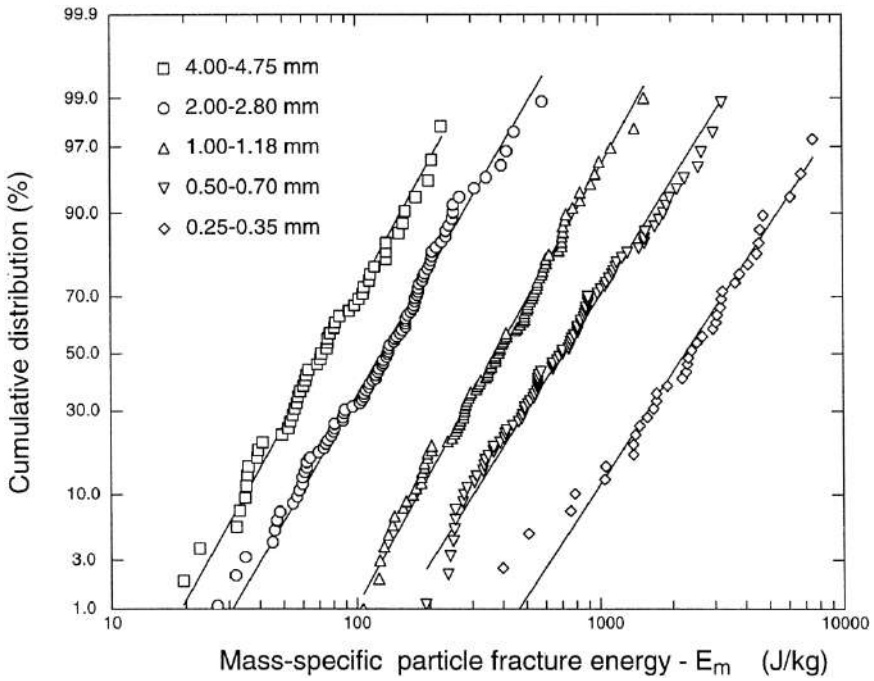

Figure II.2 – Fracture energy distributions for quartz particles. The lines represent the fit of the lognormal distribution (Tavares & King 1998).

II.1.2.2 Effect of particle size on breakage

As shown in Figure II.2, fracture energy can be strongly influenced by particle size, with a reduction in the mean particle size resulting in a displacement of the distribution to larger values. This increase in strength with size reduction is commonly observed in brittle materials and is explained based on the Griffith model for brittle fracture (Austin & Concha 1994). Geological materials typically present a certain concentration of cracks, pores and grain boundaries that act as stress concentrators, resulting in cracks. Since the size and number of cracks reduces as particle sizes reduce, stress must increase so that finer particle fragmentation occurs.

Fracture energy distributions have been measured for a variety of materials in a wide range of sizes, using different equipment for individual particle breakage (Tavares & King 1998; King & Bourgeois 1993; Yashima et al. 1987; Fandrich et al. 1998; Yashima et al. 1979; Unland & Szczelina 2004). Tavares & King (1998) reported results for individual breakage in the range of 0.25 to 15 mm for different materials, whereas Fandrich et al. (1998) and Tavares & Neves (2008) with particles up to 90 mm, all using impact load cell devices (double impact). In contrast, Yashima et al. (1979) and Unland & Szczelina (2004) performed slow compression tests for particles up to 600 mm, with an effect of increased strength with the reduction in size being confirmed.

Tavares (1997) proposed a function relating the specific median fracture energy (E_{f50}) with the representative size (d_p) of the range in which the particle population is located, being given by

$$E'_{f50} = E_{f\infty}\left[1 + \left(\frac{d_o}{d_p}\right)^{\varphi}\right]. \qquad \text{II.2}$$

This function contains three parameters ($E_{f\infty}$, d_o and φ) that should be fitted to experimental data. Figure II.3 presents typical results of the effect of particle size and the fit to equation II.2.

It is known that the intensity of particle breakage depends on the type of surface since it influences the split of the impact energy among the elements involved in this event. Tavares (2004) proposed a correction to equation II.2, based on Hertz's contact theory, in order to compensate the fracture energy when the collision involves materials other than steel. This correction is given by $E_{f50} = e \cdot E'_{f50}$ with

$$e = \left(\frac{k_{steel}}{k_{steel} + k_p}\right)\left(\frac{k_{sup} + k_p}{k_{sup}}\right) \qquad \text{II.3}$$

in which k_{steel}, k_{sup} and k_p are the stiffness coefficients of steel, the impact surface and the particle, respectively. The stiffness coefficient of any material can be estimated on the basis of its modulus of elasticity (Y) and Poisson´s ratio (μ) using the expression $k = Y/(1-\mu^2)$. The stiffness coefficient of steel is typically about 236 GPa.

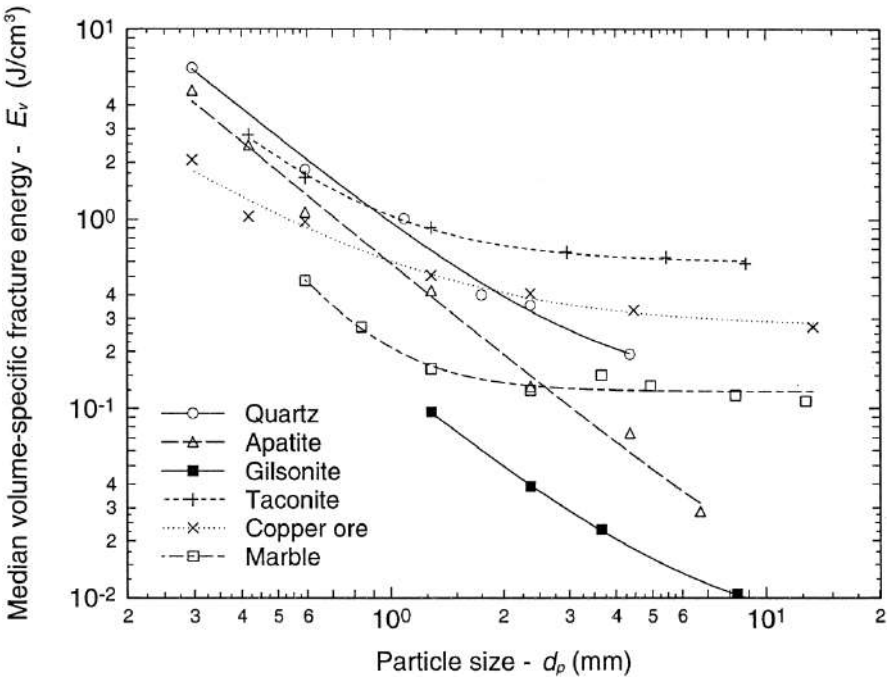

Figure II.3 – Variation of median specific fracture energy with particle size for a variety of materials (Tavares & King 1998).

In some cases, the variance of the fracture energy distribution may also vary with particle size. As such, Carvalho & Tavares (2013) proposed using a relationship similar to equation II.2 for the standard deviation of fracture energies and is given by equation II.4:

$$\sigma_E = \sigma_\infty \left[1 + \left(\frac{d^*}{d_p}\right)^\theta\right]. \qquad \text{II.4}$$

In analogy to equation II.2, the three parameters (σ_∞, d^* e θ) should be fitted to experimental data.

II.1.2.3 Fragments created after breakage

Analyzing individual particle breakage data for different energies, it is possible to observe that the higher the applied energy, the more intense breakage is and, therefore, the greater the generation of finer particles, as illustrated in Figure II.4, which shows the particle size analysis of the drop weight test (DWT) product (Napier-Munn et al. 1996) on individual particles.

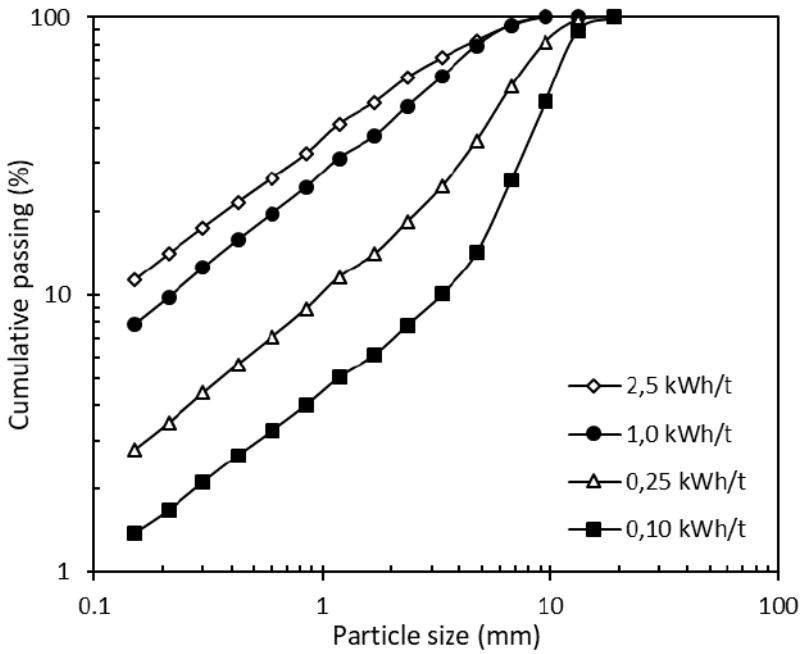

Figure II.4 – Product from DWT for a sample of granulite, for the original size of 16 x 13.2 mm in different impact energies.

Due to the complexity in the variable curvature and inclination associated to the particle size distribution curves, Whiten & Narayanan (1983) suggested its parameterization as a function of the so-called t_n parameters. The parameter t_n is defined as the cumulative passing in a size *n* times smaller than the original particle sample size. Being $d_{p,0}$ the initial size of the particle sample, it gives

$$t_n = P\left(\frac{d_{p,0}}{n}\right) \qquad \text{II.5}$$

in which $P(d)$ is the cumulative proportion in mass passing size d.

Traditionally, the parameter t_{10} is the most commonly used to describe the breaking intensity as a function of impact energy. Figure II.5 illustrates the relationship of t_{10} with

the impact energy applied to the particle (E_{cs}) for the curves shown in Figure II.4. This relationship can be described by an exponential function (Tavares, 2009) of the type,

$$t_{10} = A\left[1 - exp\left(-b'\frac{E_{cs}}{E_{f50}}\right)\right] \qquad \text{II.6}$$

where E_{cs} is given in J/kg and t_{10} in given in percentage points. Parameters *A* and *b* must be calibrated from tests on the sample.

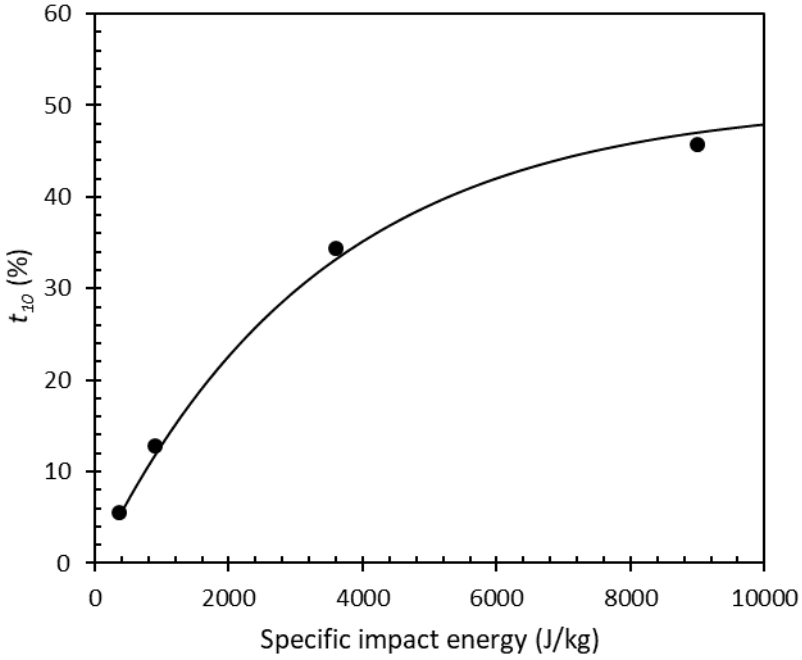

Figure II.5 – Relationship between t_{10} and specific impact energy E_{cs} for a granulite sample.

The relationship of t_{10} with impact energy describes the intensity of breakage but does not allow determining the breakage function or the reconstruction of a particle size distribution. In order to obtain a breakage function and predict the distribution of fragments as a function of the applied energy, it is necessary to use additional t_n's as a function of t_{10}. Figure II.6 presents the t_n's versus t_{10} for the data contained in Figure II.4, for t_2, t_4, t_{25}, t_{50} and t_{75}.

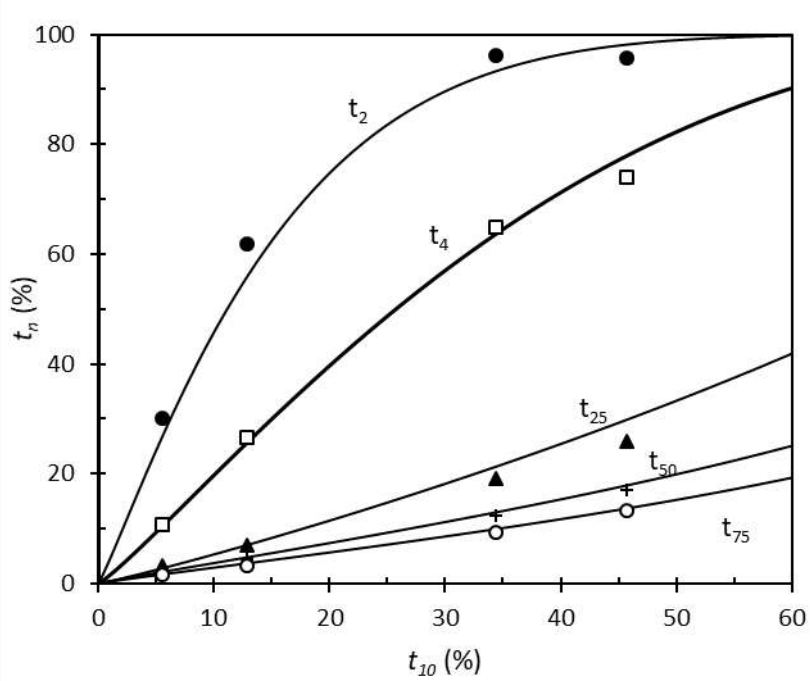

Figure II.6 – t_{10} versus t_n 's for a granulite sample. Fitted lines correspond to the incomplete beta function.

It is common to use cubic spline curves in data interpolation from points t_{10} vs. t_n, but incomplete beta functions and truncated Rosin-Rammler can be applied, providing a good fit to the data (Tavares 2007). Carvalho et al. (2015) proposed an incomplete beta function calibration methodology that prevents crossing the curves. Such crossing would represent the creation of a higher total mass of the fragments than that of the original particle, which would represent an aberration. The curves presented in Figure II.6 were fitted applying this methodology.

II.1.2.4 Damage mechanics

In industrial equipment, there is little control over individual impacts, so that the energy applied to the particle may, in some cases, be lower than the minimum necessary to cause breakage. This energy, however, may be sufficient to weaken the particle, requiring less energy in subsequent impacts for its fragmentation.

Tavares & King (2002) suggested that this phenomenon occurs through the propagation of pre-existing cracks. During repeated impacts, pre-existing defects in the internal microstructure of the particle grow until they reach critical concentration or size, resulting in breakage of the particle. Figure II.7 illustrates the growth process of pre-existing defects as a result of n repeated stressing events.

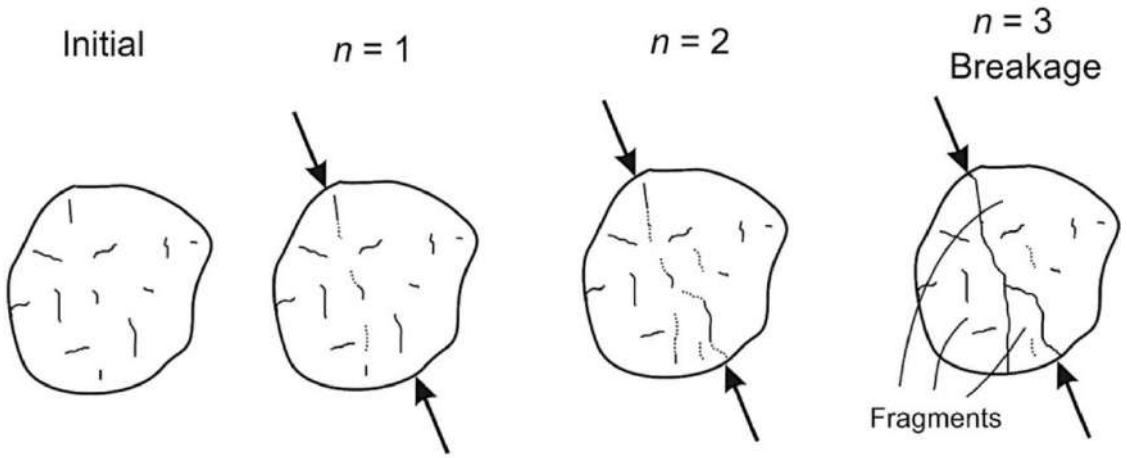

Figure II.7 – Illustration of particle weakening by damage accumulation under repeated impacts (Tavares 2009).

Tavares (1997) proposed a model based on Hertz's contact theory and damage mechanics to describe fracture energy reduction as a consequence of *n* impacts. The proposed model establishes the evolution of fracture energy as a function of the damage (D) suffered by the particle, given by

$$E_{f,n} = E_{f,n-1}(1 - D_n). \qquad \text{II.7}$$

The amount of damage suffered by the particle in the n-th stressing event is estimated by,

$$D_n = \left[\frac{2\gamma}{(2\gamma - 5D_n + 5)}\frac{E_{k,n}}{E_{f,n-1}}\right]^{\frac{2\gamma}{5}} \qquad \text{II.8}$$

where $E_{k,n}$ is the impactor's kinetic energy for a double impact on the n-th impact. The application of the model requires simultaneous solution of equations II.7 and II.8. Since D_n is implicit in equation II.8, an iterative procedure is used that typically converges in a maximum of 10 iterations from an initial estimate with $D_n = 0$. Figure II.8 presents a typical result of a repeated impact test for different materials, in which the impact energy is lower than the fracture energy.

A clear advantage of the proposed damage accumulation model is the adoption of only one parameter (γ) that needs to be fitted from repeated impact tests, whose methodology is presented in the publication of Tavares & King (2002).

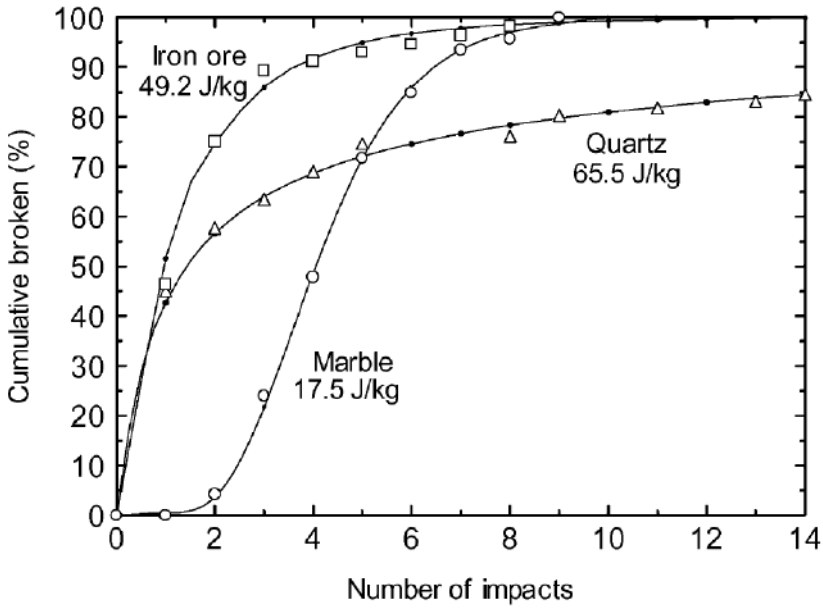

Figure II.8 – Cumulative experimental and simulated percentage after consecutive impacts for different materials (Tavares & King 2002).

II.2 Discrete element method (DEM)

For a better understanding of the comminution processes and for the proper application of the breakage models mentioned above, descriptions of the energy transfer regime for the ore particles inside the equipment must be available. The Discrete Element Method (DEM) is presented as the most suitable tool for achieving this.

II.2.1 Introduction

DEM is a numerical technique for simulating motion and interaction between discrete bodies. Fundamentally, DEM solves Newton's equations of motion in order to describe the motion of particles and applies contact models to describe the interaction forces between them. The contact models describe the collision mechanics between two or more bodies or between particles and the geometry that surrounds them. Originally, DEM was developed for studies in soil mechanics, however, initially only for a small number of particles (Cundall & Strack, 1979). In the minerals industry, the first application was carried out a few years later in the simulation of the motion of the grinding media in ball mills (Mishra & Rajamani 1992).

Considering the mechanistic modeling, DEM is able to provide the following information on the mechanics of the comminution processes (Weerasekara et al. 2013):

- impact energy distribution;

- collision rate;
- types of collisions;
- residence time;
- transport and discharge from the equipment.

II.2.2 Contact models

Various types of contact relationships are available for description of the interactions between particles. These models establish contact between smooth, spherical, non-spherical, cylindrical and non-cylindrical elastic particles, with friction and surface adhesion (Mishra 2003).

Given that the forces involved in a contact are determined by the incident velocities and the elasticity of colliding bodies, the contact model dictates whether or not the collision mechanics is an accurate representation of the physical system. Although several contact models have been proposed for use in DEM simulations, most are variations of three approaches (Zhu et al. 2007):

- Linear spring and dashpot;
- Hertz-Mindlin;
- Walton and Braun.

The theory behind these contact approaches was well summarized by Zhu et al. (2007).

The Hertz-Mindlin contact model has been used by a large number of researchers in conducting DEM simulations of mills and crushers (Tavares & Carvalho 2010; Khanal & Morrison 2008; Misra & Cheung 1999; Johansson et al. 2016; Quist & Evertsson 2016; Cunha et al. 2013; Barrios & Tavares 2016). Hertz (1882) initially proposed a theory to describe the elastic contact between two spheres in normal direction, considering that the relationship between the normal force and the normal displacement is nonlinear. On the other hand, Mindlin & Deresiewicz (1953) proposed a general model for the tangential force. They demonstrated that the force-displacement relationship depends on the entire loading history and the instantaneous rate of force variation and normal and tangential displacement. However, due to its complexity, the Hertz-Mindlin model requires intense computational effort in simulations of granular flow, which usually involves a large number of particles.

The key parameters for applying this model are the restitution coefficient and the friction coefficient. The restitution coefficient can be defined as the ratio of particle velocities immediately before and after the collision event. These parameters are intrinsic properties of the material, depending on the material of the bodies in contact, the geometry of the surfaces and the impact velocity (Johnson 1985), making its measurement and experimental determination a difficult task.

The treatment of contact between non-spherical particles is much more complex. Two techniques have been adopted to deal with irregularly shaped particles. One is to replace the non-spherical particle with a spherical particle cluster (Barrios et al. 2013; Marigo & Stitt 2015; Majidi et al. 2015; Zhao et al. 2016). The advantage of this technique is that it can be used to represent complex shapes, dealing only with contact models for spherical particles. The alternative technique is to consider particles that have other regular shapes, such as ellipsoids, polygons and cylinders, and determine whether or not there is contact between two neighboring bodies, solving their mathematical formulations (Cleary & Sawley 2002; Langston et al. 2004; Delaney et al. 2010). The contact force model used in these techniques is, in general, a modification of that adopted for spherical particles.

Although real particles often have irregular shapes, their modeling from spheres is traditionally adopted and offers computational benefits because:

- are easy to characterize;
- contact detection is simplified;
- contact models are available in the literature;
- contact can be modeled as a single point.

Given its simplicity, the use of spheres in DEM simulations is suitable for the study of the global kinematics of a large number of particles in a comminution process. However, the idealized nature of contact models does not allow a detailed analysis of individual contact events (Weerasekara et al. 2013). In fact, the results obtained should not be interpreted as accurate in terms of their physical significance. Instead, the results should be used pragmatically in order to provide average rates, frequencies and distributions of collision events for a particle population.

II.2.3 Collision energy distribution

The total energy dissipation associated with the interactions between the particles can be calculated using the contact relationships in DEM, with normal and tangential

components. It is important to emphasize that the results depend on the contact model adopted and on the assumed simplifications. The energy losses of all individual events (collisions) can be recorded to form a frequency distribution of these energy losses or dissipations, in both normal and tangential directions. In this way an energy spectrum can be calculated for each type of collision and each material class or size. Figure II.9 shows a spectrum of energy dissipated in collisions in a ball mill loaded only with grinding media. The spectra of different types of collisions are compared, allowing a more detailed analysis of the dynamic environment in the equipment.

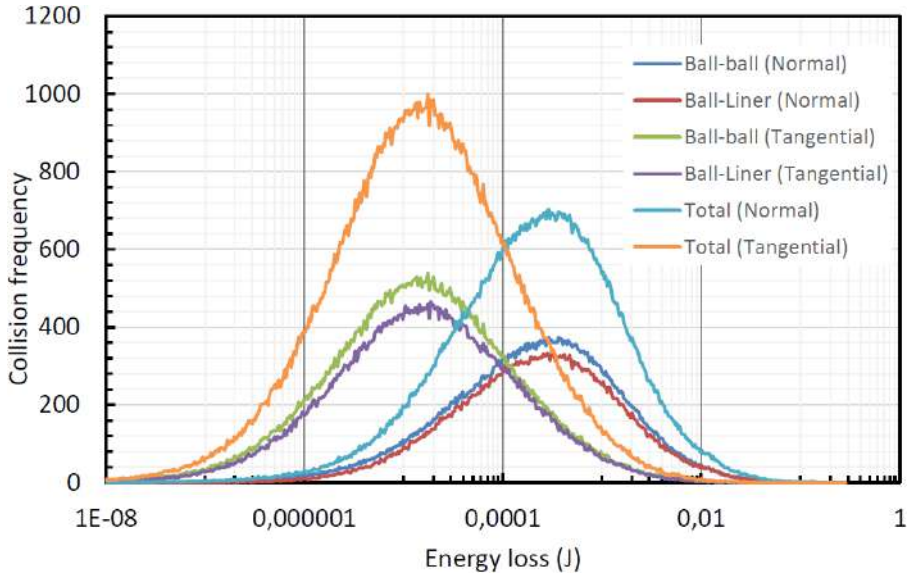

Figure II.9 – Spectrum of energy dissipated from collisions in a ball mill (Carvalho 2013).

In mechanistic modeling coupled with DEM simulations, the collision energy spectrum is represented by the dissipated energy, total or normal, instead of the kinetic collision energy. This is consistent with the assumption that only part of the kinetic energy involved in the collision is absorbed by the particles, which was experimentally confirmed by Narayanan & Whiten (1988), Tavares (1999) and Bbosa et al. (2006). However, the use of dissipated energy creates an additional complexity in the calibration of parameters used in DEM, since this type of energy is more sensitive to the choice of parameters and the contact model adopted than the kinetic energy. Thus, the calibration of parameters for simulations of comminution processes requires greater attention.

II.2.4 Breakage in DEM

DEM simulation of some comminution equipment, such as jaw and cone crushers, presents some additional challenges, as the material flow inside requires fragmentation to occur. In addition, the performance and energy consumption of the equipment may depend on the breakage and size of the fragments generated. Thus, some models of dynamic particle breakage, in DEM environment, have been proposed and are presented as follows.

II.2.4.1 Tetrahedral elements model (TEM)

Potapov & Campbell (1996) proposed a model in which the particles inserted in the DEM environment have an internal structure formed by a tetrahedral mesh, constituting a cluster of bound sub-particles. These connections are capable of resisting tensile forces up to a specified limit. Once this limit is reached, the bond is broken. According to the distribution of stresses along the volume of the macroparticle, some bonds are broken, simulating the propagation of a crack and generating fragments from the still-bound sub-particles. Figure II.10 (left) illustrates an example of a spherical macroparticle modeled by a cluster of tetrahedra. The figure also illustrates (right) the fragments generated after their collapse by compression.

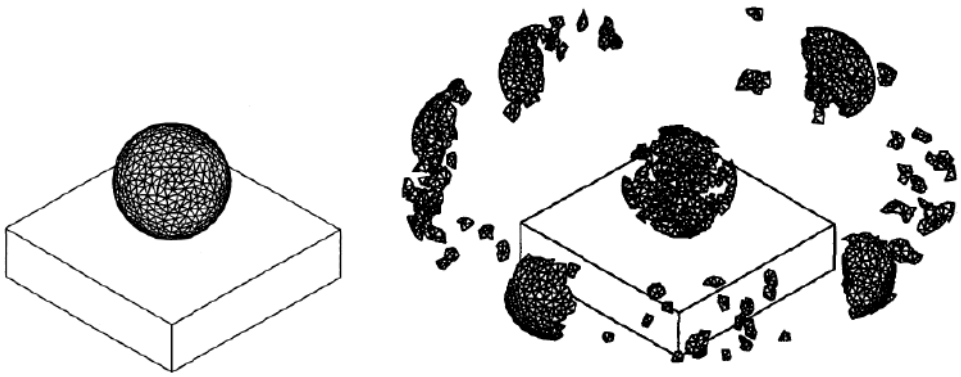

Figure II.10 – Sphere decomposed into tetrahedrons (left), and fragments produced after compression breakage (right) (Potapov & Campbell 1996).

One of the first applications of this model was in the fragmentation of free-fall spherical particles and in unconfined beds (Potapov & Campbell 1994; Potapov & Campbell 2000; Potapov & Campbell 1997). The model was also applied, using 2D squares, to the simulation of mass loss by friction in a shear cell. Despite the qualitatively similar results

to those visualized for brittle materials, these results were not compared to the experiments. Herbst et al. (2008) used data from weight loss tests in the calibration of parameters in the tetrahedral elements model, obtaining good agreement between the experimental and simulated results for a kimberlite ore. The model of tetrahedral elements was also applied to the cone crusher and the semi-autogenous grinding mill with product distributions in very good agreement to the experimental ones (Herbst & Potapov 2004; Lichter et al. 2009).

Although the particle size distributions from the studies mentioned above presented good agreement, in some cases qualitative and in others even quantitative, to the experiments, no comparisons of the strength vs. deformation profiles and the energy consumption in particle breakage were found in the literature. Thus, the verification of the reliability of the model of tetrahedral elements as to the energy distribution and to the appropriate description of the microbreakage processes still needs to be studied more deeply, being the object of ongoing research at LTM (Jiménez-Herrera et al. 2018).

Despite the versatility offered by the model when adopting tetrahedrons in the representation of mineral particles, enabling the formation of angular fragments, this approach adds complexities to the simulation algorithm, considerably increasing its computational demand. While a sphere requires only two parameters for its characterization (position and diameter), tetrahedrons require the position of each vertex. If a non-regular tetrahedron is considered, additional parameters are then needed. Thus, two steps of the algorithm become more complex: the detection of the contact between the elements and the calculation of the volume of the tetrahedrons overlap during the collision, necessary in the calculation of the resulting force and energy dissipated in the event. Cundall (1988) demonstrates the additional effort inherent to the adoption of tetrahedron in DEM simulations.

II.2.4.2 Bonded particles model (BPM)

As an alternative to the use of tetrahedra, Potyondy & Cundall (2004) proposed a model similar to that of Potapov & Campbell adopting the use of spheres. Figure II.11 illustrates an agglomerate of bound spherical particles forming a mother particle. The authors argue that a rock behaves as a cemented matrix granular material, where both particle grains and bonds are deformable and can break. Also, according to the authors, this conceptual model would explain all aspects of the mechanical behavior of the material. This approach presents an advantage in its computational requirement, since, by using only spheres, the detection and resolution of contacts is simplified.

The BPM allows, in theory, adoption of daughter particles according to a distribution of size and association of different properties to different regions of the internal volume of the mother particle. The use of a daughter size distribution allows the fragments generated to follow a predefined distribution in the breakage event. On the other hand, the use of different properties in subgroups of daughter particles allows the simulation of different grains inside the mother particle and orientation of the crack propagation, in order to make fragmentation outcome closer to that observed in practice. It is important to emphasize that more complex and detailed modeling of its particle requires a more detailed characterization of the simulated material, besides the computational penalization of the simulation.

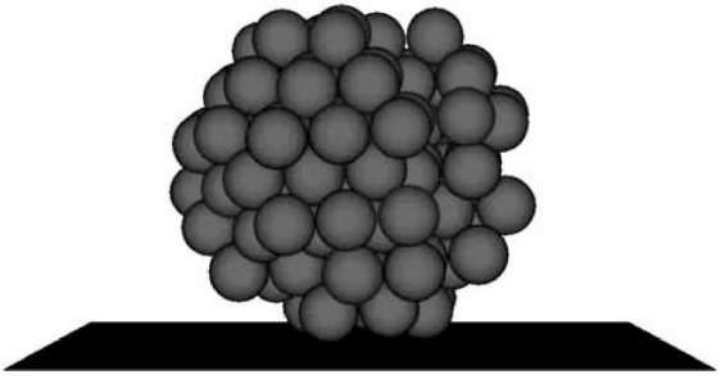

Figure II.11 – Agglomerate of bonded spherical daughter particles (Lim & McDowell 2005).

In its original formulation, proposed by Potyondy et al. (1996), the contact between two particles occurred in only one point aligned with both centers. Cho et al. (2007), however, modified this contact to a region of connections, emulating a cemented connection, thus obtaining, for compression tests, stress-deformation profiles with excellent correspondence to the experiments. Spettl et al. (2015) used a stochastic model to generate random and isotropic microstructure clusters, obtaining variability in their fracture energies. The study observed that the volume of the two largest fragments obtained after breaking, which occupied on average 83% of the total volume, was very little influenced by the size of the particles inside the agglomerate.

The bonded particle model was successfully applied in the simulation of cone crushers (Quist & Evertsson, 2016; Johansson et al., 2016), predicting the product size distribution with good agreement to experiments. Legendre & Zevenhoven (2014) used the model to predict the energy consumption of a jaw crusher.

II.2.4.3 Particle replacement model (PRM)

Both the model of tetrahedral elements and the model of bonded spheres present the disadvantage of the need to simulate the sub-elements of each macro particle throughout processing, considerably increasing the computational cost of the technique.

In order to overcome this disadvantage Cleary (2001) introduced an alternative that consists of identifying the conditions where a particle would fragment and then replace the original particle with a set of daughter particles agglomerated in the space previously occupied by the parent particle. In this way, the fragments would appear in the simulation only after breakage occurs. Figure (II.12) illustrates the process of particle replacement after fragmentation. Breakage or substitution can result from application of either criterion:

- Particles are broken if the accumulated dissipated energy, during a collision, exceeds a fracture energy dependent on its size;
- Particles are broken if the total instantaneous force applied exceeds a size-dependent value of compression force.

Recently, Delaney et al. (2010) extended the technique to the adoption of non-spherical particles, with a fragments packing methodology that is responsible to create variability among breakage events. However, so far the methodology proposed in the study does not guarantee a size distribution of the fragments related to the energy involved in the impact.

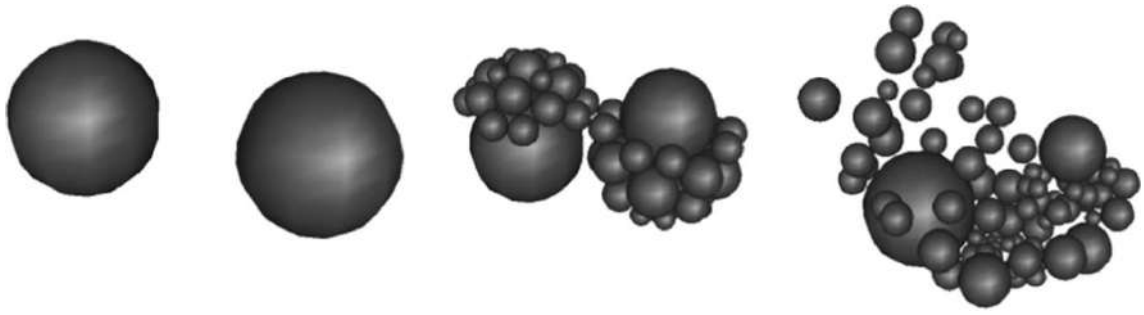

Figure II.12 – Breakage of two colliding particles. (a) before impact, (b) immediately after impact and (c) free fragments (Cleary & Sinnott 2015).

The main advantage of the PRM is the lower computational demand, since a smaller number of particles is necessary to describe the population in comparison with the other two methodologies of dynamic breakage in DEM environment. On the other hand, it presents some critical issues that directly affect the results, such as the number and size

distribution of daughter particles and packing within the original volume of the parent particle.

Unlike the bond-based models, for PRM, after breaking all particles will be free, so that their size should directly represent the size of the real fragments. However, a realistic number of daughter particles must be adopted in order to maintain the computational benefit of the technique. An adequate balance should then be defined between the number of daughter particles and their size in order to maintain consistency with experimental data. The packing of the fragments in the space left by the original particle is a possible source of disturbances in the simulation and will be treated in more detail in the next section.

Some practical applications present great challenges of DEM simulation without considering breakage, among them is the problem of compression of confined beds. Barrios & Tavares (2016) modelled a roller press, applying the particle replacement model, demonstrating the difficulty of achieving realistic predictions without considering breakage in DEM. Due to its reduced computational effort, the PRM was applied using a fractal size distribution, to different types of compression crushers, such as jaw, gyratory, cone and roller crushers (Cleary & Sinnott 2015), and to impact crushers, such as hammer, vertical and horizontal shaft impact crushers (Sinnott & Cleary 2015), already Delaney et al. (2015) used superquadratic shaped particles in the simulation of a cone crusher.

II.2.4.3.1 Particle packing

The three methodologies presented in the previous sections present a similar problem: how to model the mother particle from the daughters? Considering that each real ore particle breaks differently, the adoption of a single pre-set or overly simplified packing can result in a bias in the size distribution of the final product. An ideal algorithm should ensure the following properties to a daughter particle cluster: high coordination number, isotropy, ability to occupy arbitrary boundary volumes and absence of internal stresses.

As observed by Potapov et al. (1995) the use of equilateral triangles in the model of tetrahedral elements, in 2D, results in a too perfect crystal, with its breakage generating symmetric fragments in relation to the direction of impact. However, when using Delauney's triangulation to generate the triangle structure inside the cluster, providing randomness to the crystal matrix, a brittle behavior was verified in its fracture. Then Potapov & Campbell (1996) demonstrated that this structure, with properly calibrated connections, provides results that are compatible with experimental data.

For the model of connected spheres, it was demonstrated that a bimodal distribution of particle size provides high packing density, maintaining the desired properties of the agglomerates (Brouwers 2006; Groot & Stoyanov 2011). Similarly, Quist & Evertsson (2016) applied the bimodal distribution in the creation of bead agglomerates, obtaining brittle fracture and a size distribution compatible with experimental data in a cone crusher.

In the case of the particle replacement model, some additional precautions should be taken, since the fragments are not originally present in the simulation and their insertion should not disturb it. Obviously, the total mass should be maintained during the fragmentation and the choice of the distribution and positioning of the fragments should be based on the following criteria:

- the number of fragments generated should be relatively small in order to enable simulation;
- size distribution and packing should be chosen so as to reduce local pressure after breakage;
- the breakage mechanism should, as far as possible, emulate the real particle breakage.

Meeting all the criteria simultaneously is very difficult and some concessions must be adopted.

Ciantia et al. (2015), in simulations of coke compression adopting a fractal distribution of beads with decreasing sizes, found that from a certain number of particles there was no significant variation in the macro-mechanical response of the sample. On the other hand, the choice of the minimum particle size that is allowed to break influenced both the distribution of the final product and its mechanical properties. In another study, Li et al. (2014) realized that the particles of a rock sample, when compressed, broke into two pieces of similar mass, and fine fragments with, in total, less than 10% of the mass of the original particle were generated. Thus, a simple substitution, such as two or three fragments, preserving the original mass, could be adopted. However, more complex arrangements have also been adopted. Cleary & Sinnott (2015) applied, in the simulation of some crushers, the arrangement illustrated in Figure II.12, with size distribution in which the diameter of the largest fragment is a function of the energy dissipated in the breakage event and the size of the finer fragments is chosen in order to fill the volume of the original particle. Although a more complete size distribution is produced at the end of the process, due to the methodology adopted, it was not able to represent the breakage behavior observed in ores.

Delaney et al. (2010) proposed an interesting dynamic packing methodology, which consists of creating, within the volume of the original particle, a series of "seed" particles with a fraction of the desired size and following a defined distribution. These seeds grow in size at a constant volumetric rate. As they grow and fill the limit volume, the interaction between them is allowed so that they push, with zero friction, and organize themselves in the internal space of the original particle. This dynamic is interrupted when the packing density reaches equilibrium. Figure II.13 shows a diagram of this process. One of the advantages of this approach is to add variability in fragmentation, both in the positioning of the fragments in the final arrangement and their orientation. However, the formulation currently proposed by the authors does not guarantee that the final distribution of the fragments follows a desired distribution to simulate a real process. This methodology was applied to the simulation of a cone crusher, demonstrating the ability to predict the distribution of the final product, however no comparison with experimental data has been presented (Delaney et al. 2015).

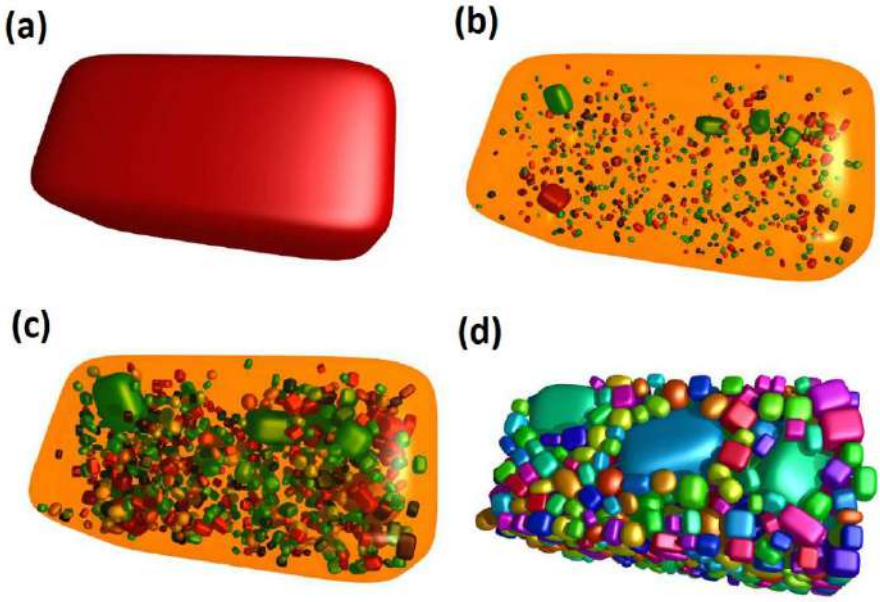

Figure II.13 – Scheme of the stages of the packing process proposed by Delaney et al. (2010). (a) original particle, (b) seed creation, (c) fragment growth and (d) final arrangement.

Barrios et al. (2015), on the other hand, applying the t_{10} model in determining the distribution of fragments, circumvented the problem of packing allowing the intensive overlap between the particles generated. In order to prevent an explosive decompression of particles, the Hertz-Mindlin model was modified by inserting a dissipation coefficient,

maintaining the stability of the simulation. However, other micro-processes related to the breakage of mineral particles, presented in section I.1.1, were not considered.

II.2.4.4 Second generation and hybrid breakage models

Starting from the three approaches descried above, some authors proposed modifications in them in order to simulate reliably the complexity of fracture. Barrios et al. (2015), using particle replacement, adopted the t_{10} model to define fragments generated after breakage. On the other hand, the total particles mass was not conserved, with the selection of a minimum size to be created in the mass below this size simply being lost. Additionally, particles can only break a single time, without breakage of fragments. In this work, the criterion of breakage was the maximum applied force measured by compression of individual real ore particles. In the simulation of the compression of a confined bed of iron ore pellets, that possess high sphericity, the authors obtained very good results in terms of compressive force profile in the bed and percentage of broken particles, as presented in Figure II.14 - top. On the other hand, the simulation could not properly predict the fragments sizes after compression for any of the applied maximum force (Figure II.14 – bottom). This can be explained by the use of a single fragments distribution and the assumption that all particles in the bed break in the exact same way.

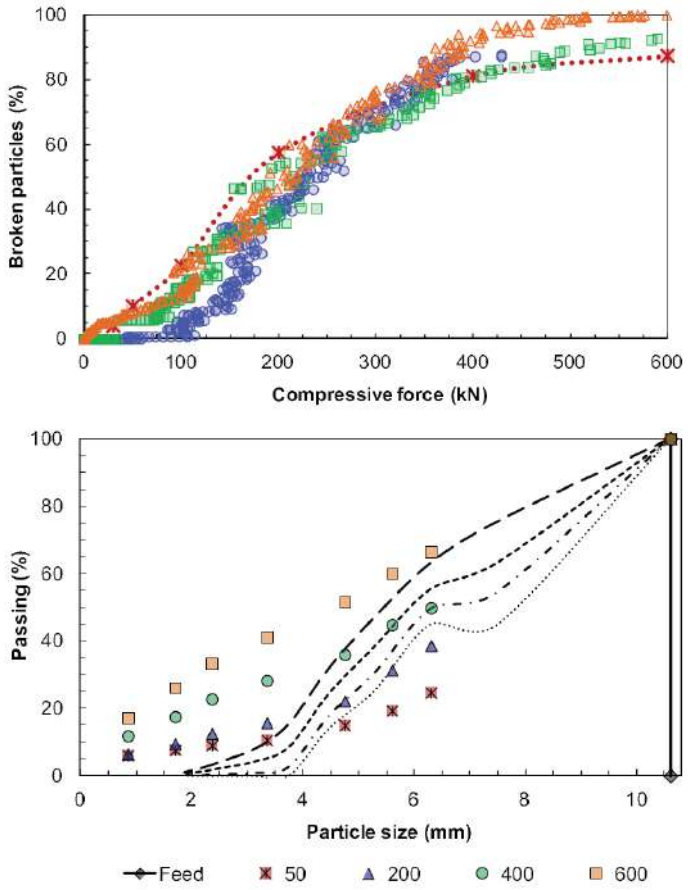

Figure II.14 – (Top) Proportion of broken particles as a function of compressive force applied, where the dotted red line is from experiments and the point from simulations. (Bottom) Size distributions experimental (symbols) and simulated (lines) of the bed of particles after different maximum compressive forces applied (Barrios et al. 2015).

Jiménez-Herrera et al. (2018) analyzed particle breakage using three models available in commercial DEM simulation platforms: the bonded-particle model (BPM), the particle replacement model (PRM) and the fast-breakage model (FBM). The three techniques were used to simulate breakage of copper ore particles in unconfined beds by a free-falling steel ball. More relevant to this work is the comparison between PRM and FBM. The particle replacement model adopted was the same develop by Barrios et al. (2015), discussed above. The fast-breakage model is a hybrid of the PRM and the Tetrahedral elements model, with the main difference being that particles are non-spherical and the fragments replace the primary particles. Additionally, in the FBM the fragments sizes follow a simplified version of the t_{10} model and the total mass is conserved by artificially adding the missing mass, that would be generated bellow a minimum size, into coarser sizes. Figure II.15 illustrates the modes of breakage.

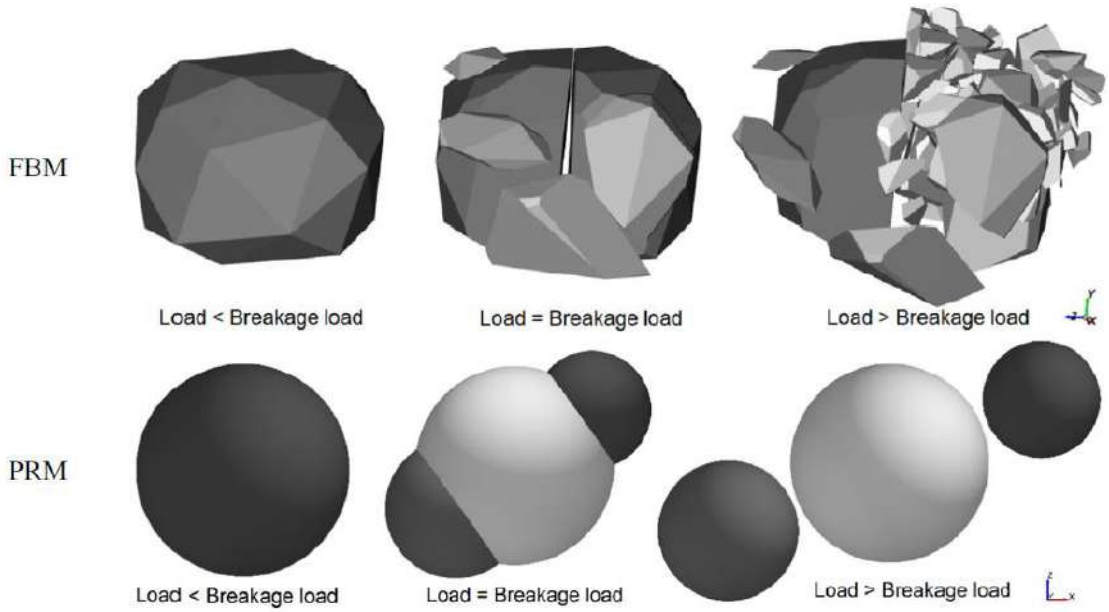

Figure II.15 – Comparison of the breakage steps between the particle replacement model (PRM) and the fast-breakage model (FBM) (Jiménez-Herrera et al. 2018)

In terms of the number of broken particles as a function of bed diameter (represented by the number of rings of particles), both techniques obtained very similar results, although overestimating the broken mass for bed diameters bigger than one ring of particles, as presented in Figure II.16 (top). This might be associated with instantaneous nature of breakage in both models, which creates a less-than natural response of the particle bed as particle break. This is evident after breakage of the first particles in the bed so that immediately after this moment the advance of the ball is less restricted, allowing for the steel ball to penetrate deeply in the bed, causing more breakage. In the future, this could potentially be avoided by dissipating the kinetic energy of the impactor during contact.

Looking at size distributions of the fragments, the particle replacement model developed by Barrios et al. (2015) could predict the experimental data very effectively up to the minimum size. In contrast to the previous application (Figure II.14), where this technique was not as effective in predicting fragmentation, in this case, breakage of a monolayer unconfined particle bed is a simpler configuration than a multilayer confined bed compression, where not only the multiple contacts with the geometry, but also particle-particle contacts, must be resolved. This version of the technique seems to not represent all complex mechanism of fracture for such a complex scenario as that of Figure II.14. On the other hand, the fast-breakage model (FBM) overestimated fragmentation after impact, which was expected considering that the technique conserves the total broken mass by artificially adding mass into coarser size fractions.

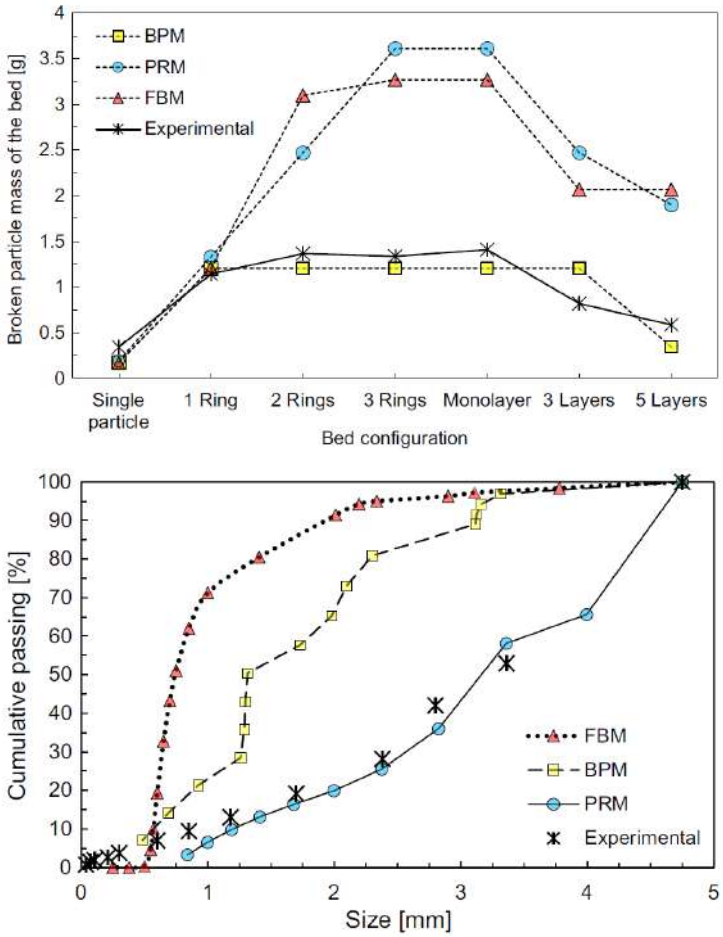

Figure II.16 – Comparison between experimental and predicted broken particle mass and progeny size distributions broken out of the narrow size (breakage function) for an impact of an 88-mm diameter steel ball at an energy of 3.0 J on copper ore particles (Jiménez-Herrera et al., 2018).

In a very recent work, Tavares et al. (2020) improved the fast-breakage model (FBM) by adapting more of the breakage phenomena discussed previously at the commercial DEM package Rocky DEM. Micro phenomena such as size-dependent breakage probability distribution, particle weakening by repeated stressing events and energy-dependent fragment size distribution were implemented, resulting in very good breakage results compared with experiments. Figure II.17 presents fragments size distributions curves for simulations and experiments of a free-falling steel ball on an unconfined particle bed.

The DEM package selected for this work simulates real particles by tetrahedral shapes, making it a hybrid of the TEM and PRM. The primary particles were simulated without smaller bonded fragments and, after breakage detection, they were replaced by tetrahedral smaller fragment particles. This choice allowed the elimination of the

overlapping volumes after replacement, however limited how small the fragments can be. Keeping in mind the computational expenditure during the contact detection calculation when using non-spherical particles, the concomitant simulation of coarse and fine particles (1/10 size ratio) start to require a fairly large computation time. For this reason, as can be noticed in Figure II.15, the authors only simulated up to sizes about 1/8th of the original parent particles. Thus, simulations of long and discontinuous processes, such as batch milling, would tend to deviate from the experimental data.

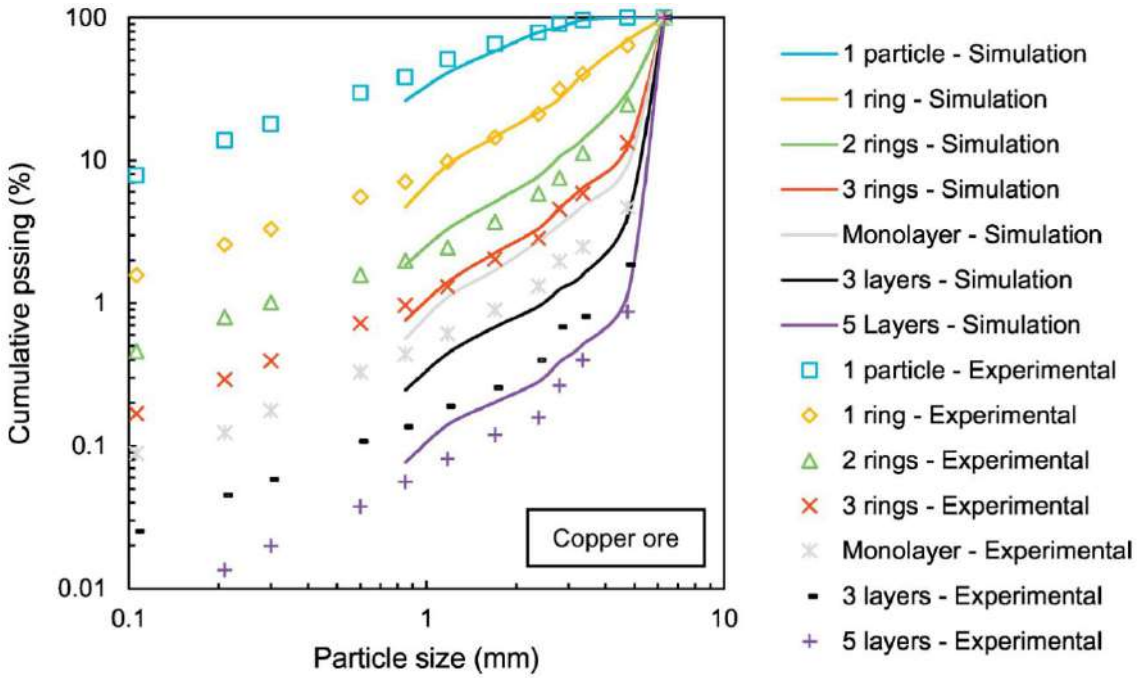

Figure II.17 – Comparison between size distributions of the particle bed material after impact of a steel ball (Tavares et al., 2019).

It is possible to recognize that, among the different methods reviewed, the particle replacement method is the one that best suits the needs of application to comminution systems, in view of its higher computational efficiency. However, there is no consensus on the best form of its application in order to ensure good correspondence to experimental results.

III. MODEL DEVELOPMENT AND IMPLEMENTATION IN DEM

The methodology developed and presented in this document incorporates much of what was learned over the last 20 years or so on particle breakage, which is available in the published literature. Although it was based on the Particle Replacement Model (Cleary, 2001), presented previously, it is called here as “DEM particle breakage” model since it goes well beyond describing breakage by replacing a particle by its fragments, as will be evident as follows.

The DEM particle breakage model incorporates the microprocesses and equations related to brittle breakage of hard particles into the DEM algorithm scheme. In spite of being complex, the model is thought as the most general possible, requiring a comparatively small volume of calibration studies, most of which already standardized or in the literature or easily adapted to the user requirements.

For this work, the DEM particle breakage model was implemented in the form of an Application Programming Interface (API), in collaboration with the company DEM Solutions (Edinburgh, UK) into the commercial software package EDEM®. The Hertz-Mindlin contact model, described in section II.2.2, was selected to describe interaction between particles and with them with the geometry.

The main philosophy of the DEM particle breakage model is that a particle, of some brittle material, breaks when the stressing energy applied to it exceeds a critical value, called particle fracture energy (E_f) and it is an intrinsic property of the individual particle. As discussed in section II.1.1, The fracture energy is strongly influenced by the size of the particle, with the reduction of the particle size resulting in an increase of the energy required to break the particle. On the other hand, even within the same size range, particles present different fracture energies, even with the same composition and source.

In order to realistically describe breakage of brittle particles, the following concepts were implemented:

- The particle will break when the total energy dissipated in a collision exceeds a critical value;
- For a given material, particles of the same size have different breakage criteria, following a statistical distribution;
- The value of the breakage criterion, intrinsic to the particle, decreases when the particle suffers a collision of less magnitude than the previous value of the criterion, due to a weakening effect;
- Particles break into a set of fragments, with size distribution dependent on collision energy;

- The fragments generated will have their own breakage criteria, following a distribution, but independent of previous events related to the “mother particle”.

Before the start of a simulation, using the DEM particle breakage model, the user must provide a series of input parameters that regulates the microprocesses related to real particle breakage for the simulated material.

III.1 Particle creation

In order to track the breakage behavior of particle in real-time during a simulation, the developed API assigns new intrinsic properties to each individual particle.

When new particles are created in a simulated environment, the API assigns a fracture energy (E_f) value for each particle based on its material and diameter. During simulation E_f is used as breakage criterion. The value of E_f of a particle is assigned using a random number generator, already available in the EDEM code library, that follows the log-normal probability function, given by equation II.1. The E_f generator uses as input the median fracture energy (E_{f50}) and the standard deviation (σ_E). Equation II.2, presented in section II.1.1.2, demonstrates the relationship between E_{f50} and particle size. Considering that the software EDEM simulates only spheres, the particle size is equal to its diameter. The material parameters $E_{f\infty}$, d_o, φ and σ_E are inputs from the user. The unit of the fracture energy and E_{f50} is J/kg.

The lognormal function has no theoretical upper limit for its domain values. As such, in order to avoid the creation of unrealistically tough particles, E_f may assume any value up to four times E_{f50}, thus defining a practical upper truncation.

As the result of adoption of the random generator, with an account for the particle diameter and the material properties, the description of variability in breakage criteria among particles of same size, as observed in real particles, becomes possible. Moreover, the inclusion of equation II.2 to describe E_{f50}, additionally promotes the relative increase of particle strength with size class.

III.2 Procedures during simulation

The DEM procedures related to simulation of particle motion were not changed, with the calculation done by the API occurring only during and after simulated collisions between two particles and a single particle with a geometry.

After the end of each simulated contact, the EDEM software provides a value of the dissipated kinetic energy (E_{loss}) between two elements, e.g. particle-particle and particle-geometry, in which E_{loss} is a function of material and contact properties of the two elements. It was assumed that the only energy available to cause plastic deformation in a particle, and therefore breakage, must be equal or smaller than E_{loss}. From the E_{loss} value an effective energy for breakage is calculated and compared to the particle fracture energy (E_f).

III.2.1 Effective energy and breakage detection

During a simulation, most of the contacts detected are related to particles solely touching each other and with values of energy dissipation that are too small to reach any inelastic deformation. With that in mind, the user can select a minimum (E_{min}) value of E_{loss} that will engage the API procedures. For $E_{loss} < E_{min}$, calculations described as follows are skipped, thus saving computational effort.

The EDEM software additionally provides the normal (E_{norm}) and tangential (E_{tang}) components of the dissipated energy and the individual contribution of each was considered in the model formulation. These component contributions, c_n for E_{norm} and c_t for E_{tang}, to the effective energy, may be defined by the user.

During simulation, after a collision is finished and the E_{loss} value calculated, the API calculates the effective energy (E_{ef}), in Joules, based on the two elements involved, according to:

a) Collision between particles of the same material – each particle receives the same amount of effective energy, according to

$$E_{ef} = \frac{1}{2} \cdot \left(c_n \cdot E_{norm} + c_t \cdot E_{tang}\right) \quad \text{(III.1)}$$

b) Collision between a particle and surface of different materials (particle-particle or particle-geometry) – each particle involved receives a fraction (e) of the dissipated energy depending of its contact stiffness (k), according to the equation below. The contact stiffness of steel can be assumed to be equal to 236 GPa.

$$E_{ef} = e \cdot \left(c_n \cdot E_{norm} + c_t \cdot E_{tang}\right) \quad \text{(III.2)}$$

$$e = \left(\frac{k_{surf}}{k_{surf} + k_p}\right)\left(\frac{k_{steel} + k_p}{k_{steel}}\right) \quad \text{(III.3)}$$

After E_{ef} calculation for an individual particle, this value is compared to the particle fracture energy (E_f). If $E_f \leq E_{ef}/m_p$ the particle is considered broken and will be replaced. If $E_f > E_{ef}/m_p$ the particle only suffers damage and E_f is reduced. m_p is the mass of the particle.

The contact stiffness (k) for the particles is calculated based on the material Poisson's ratio (ν) and modulus of elasticity (Y), according to equation III.4 (Tavares & King, 2004). Both are input parameters for DEM simulations.

$$k = \frac{Y}{1-\nu^2} \tag{III.4}$$

III.2.2 Particle damage

In the case when $E_f > E_{ef}/m_p$ and the particle does not break, the amount of structural damage (D) suffered by each particle involved in the collision event is calculated as a function of E_{ef}. For this purpose, the API uses an iteration scheme, based on Newton's method, to solve the implicit equation III.5, modified accordingly on the basis of equation II.8:

$$D = \left[\frac{2\gamma}{(2\gamma - 5D + 5)} \cdot \frac{E_{ef}}{E_f \cdot m_p}\right]^{\frac{2\gamma}{5}} \tag{III.5}$$

where γ is an input parameter provided by the user. It is important to point out that D is calculated separately for both particles involved in the collision, since each might have different values of E_f and m_p. Once D is estimated, the updated fracture energy value assigned to the particle is $E_{f,new} = E_{f,old} \cdot (1 - D)$, replacing E_f before the start of the contact. Apart from this change the particle remains intact, that is, unbroken.

III.2.3 Fragment size distribution

Considering the case in which $E_f \leq E_{ef}/m_p$ for one of the particles involved in a collision, this particle will be considered broken and a replacement procedure is initiated. The first step, however, consists in determining the intensity of fragmentation. For this, the t_{10} parameter is first calculated as a function of E_{ef} (Tavares, 2009):

$$t_{10} = A\left[1 - exp\left(-b'\frac{E_{ef}}{E_{50b} \cdot m_p}\right)\right] \tag{III.6}$$

where

$$E_{50b} = E_{f50} \cdot exp\left[\sqrt{2} \cdot \sigma_E \cdot erf^{-1}\left(F\left(E_{ef}/m_p\right) - 1\right)\right]. \quad \text{(III.7)}$$

E_{50b} represents the median particle fracture energy of the particles that would have broken by a collision of energy E_{ef}. A and b' are material parameters provided by the user. Although with the same general form as equation II.6, this formulation has demonstrated to be capable of describing the influence of particle size on fragmentation (Tavares, 2009).

As discussed in section II.1.1, brittle particles fragment in an almost chaotic form, with each individual real particle breaking with its own fragment size distribution. However, for a population of particles of the same size and material, the average fragment size distribution is constant and may be regarded as an intrinsic property of the population. A proposed solution is to adopt a number of fragment distribution sets, available for a range of t_{10} parameters, to be sampled every time a particle breaks.

These sets of fragments will be called henceforth as a “family” of fragments. Figure III.1 presents an example of families of fragments for one material and t_{10} of 2%. The diameter of the fragments or “daughter particles” are a fraction of the diameter of original or “mother” particle. The first column in Table III.1 are nine fractions of a diameter equal to 1 and represent the possible sizes in which the daughter particle can be created. Each column, from the second to the last, represents a family of fragment sets and provides the number of individual daughter particle that will be created, for the fraction size in the same line. Such families have been prepared for various values of t_{10}.

After detection of breakage, the API will follow the steps below for the replacement procedure:

1. Calculate t_{10} as a function of the particle properties and E_{ef};
2. Randomly select one of the family available for the calculated t_{10};
3. Replace the original mother particle by a group of daughter particles dictated by the selected family.

A new E_f value is assigned to each daughter particle created, following what was discussed in section III.1.1, independent of the mother particle collision history, but dependent on the size of the daughter particle.

Table III.1 – Example of 10 families of fragments for a given material and t_{10} equal to 2%

Fraction of original size	Fragment sets									
	F1	F2	F3	F4	F5	F6	F7	F8	F9	F10
0.8000	1	1	1	1	1	1	1	1	1	1
0.6400	1	1	1	1	0	1	1	1	1	1
0.5120	1	1	1	1	2	1	0	0	1	1
0.4096	0	0	1	0	1	0	1	2	0	0
0.3277	0	1	1	1	3	1	2	0	1	2
0.2621	0	2	0	2	0	0	1	2	0	0
0.2097	2	0	0	2	2	1	0	1	0	3
0.1678	0	1	0	2	0	0	2	0	0	0
0.1342	3	2	1	2	1	5	3	3	2	2
0.1074	2	4	3	3	3	2	1	0	3	3
Mass loss (%)	6,3	0,6	-1,8	-1,6	2,1	3,3	5,1	3,6	4,8	-1,5

.

This approach intends to replicate the variability of fragmentation that occurs during breakage of a real particle. The families are created prior to the beginning of the simulation, in such a way that if a large number of particles of the same size and material breaks, the combined fragments generated will be equivalent to those found in the experimentally observed data. Later in the document the algorithm for creation of the families as a function of material parameters is presented.

Assume that in a simulation, ten particles of same size and material were impacted with the same E_{ef} and suffer breakage. Considering the example in Table III.1, if the API replaces each of the ten broken particles by a different family of fragments from Table III.1, the combination of all fragments generated would result in the distribution presented in Figure III.1. Additionally, the size distribution calculated applying the impact energy to equation III.6 and the appearance function discussed in section II.1.1.3 are presented. The same parameters were used to calculate fragments distribution by the theoretical equations and to create the families in Table III.1. Due to the adoption of discrete spheres with predefined size, it is very difficult to conserve 100% of the mass of the original particles after replacement. For this reason, each family in Table III.1 might lose or gain mass in relation to the original particle. The last line of Table III.1 presents the percentage of mass lost after replacement. Considering the vast number of potential breakage events in a simulation, the overall mass loss could tend to zero in function to the complete set of families adopted.

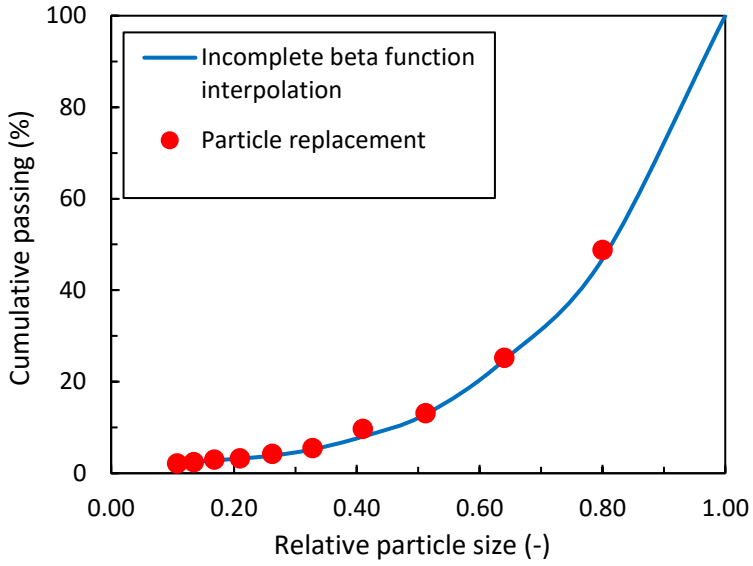

Figure III.1 – Comparison between fragment distribution calculated from the analytical equations and resulting from replacement of 10 particles by the families of fragments, for the same material parameters and applied energy (t_{10} of 2%).

III.2.4 Fragments arrangement during replacement

One large disadvantage in simulating breakage of particles using spheres is that, when dealing with particle replacement, the daughter particles are spherical as well. Considering the example in Table III.1, the largest daughter particle that can be created has 80% of the diameter of the mother particle, whereas the second largest has 64%. In most of the breakage cases, the total volume of fragments is larger than the volume of the original particle and an artificially large overlap between the daughter particles becomes unavoidable. This large overlap would cause an explosive separation of the fragments, due to the immense repulsion forces, resulting in an unrealistic motion behavior.

Barrios et al. (2015) proposed to create all the fragments in the volume occupied originally by the mother particle and allow this overlap to occur. However, a dissipation coefficient is multiplied to the repulsive force, reducing its magnitude until separation. This approach has been adopted in the present work. The dissipation coefficient was calibrated by Barrios et al. (2015) and the same value of 0.2 was used in the present work. Once free, the new particles behave as regular particles with no difference between them and other particles generated previously.

Due to inherent variability and randomness of the distribution of fragments, it is not possible to predefine the position of the new particle inside the cluster. In an attempt to qualitatively reproduce what happens during fragmentation of particles in reality, the API positions the two or three largest fragments in a plane that is orthogonal to the direction of the major stress responsible for the breakage. This has been used to induce preferential motion of the large fragments away from the point of collision. Figure III.2 illustrates this positioning. The smaller fragments are positioned randomly in the remaining voids inside the creation volume.

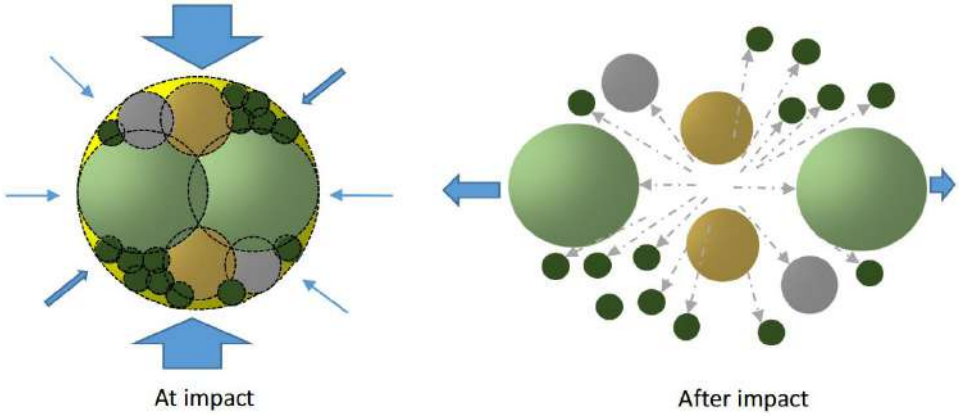

Figure III.2 – Illustration of the effect of fragment positioning inside the original particle.

III.2.5 Breakage detection for continuous contact

Considering that EDEM only determines the Collision Energy loss (E_{loss}) after a contact has ended, a change in the collision energy (E_{ef}) calculation must be done for events in which the particle fracture energy (E_f) might be reached and contact has not been lost. That situation is particularly common in some crushers, in which particles are broken under confinement.

The proposed solution is as follows. The energy absorbed by the particle during a compression (E_{comp}) is calculated using the local deformation (Def), in the point of contact, suffered by the particles and the compression force (F_c) applied to it. If it is assumed that a compression occurs in steps of time (dt):

$$dDef_i = sp_i - sp_{i-1} \tag{III.8}$$

where sp_i is the size of the particle in direction of applied force for time step i and $dDef_i$ is the infinitesimal deformation suffered by the particle. The compression energy absorbed by a particle for a time step dt is then:

$$dE_{comp,i} = F_{c,i} \cdot dDef_i \tag{III.9}$$

The total compression energy absorbed during continuous compression event would be

$$E_{comp} = \int_{t_0}^{t_f} F_c \cdot dDef \tag{III.10}$$

When applying this procedure to the numerical logic of DEM, it is necessary to consider that a particle will not actually deform, rather will overlap another surface. Consider Figure III.3 in which two overlapping particles of similar diameter appear. In reality a particle would present a contact point in the center of the overlapping area and would deform accordingly. In the logic of DEM, for particle #1 in Figure III.3, the infinitesimal compressive energy would be $dE^1_{comp,i} = dF^1_{c,i} \cdot \left(dov^1_i - dov^1_{i-1}\right)$, where ov^1_i is half of the total overlap between two particles in contact. In the case of contact with the surface of the geometry, it is assumed that no deformation occurs in the surface of the geometry, so that $dDef$ would be the total overlap of the particle into the geometry.

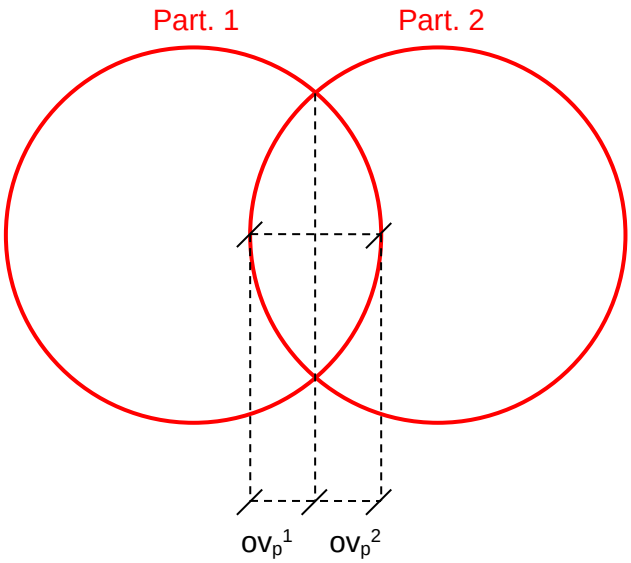

Figure III.3 – Scheme of two overlapping particles of the same size.

In the case of particles with different diameters, the deformation of one particle will continue to be the distance between the contact points of both surfaces and further point

of the second particle into the other. In this way, the E_{comp} of each particle will depend on its size in relation to the other particle.

As it is evident in the formulation presented above, this methodology assumes that the total compressive energy only increases with additional overlapping of the particles. During the contact of two bodies, dE_c must be calculated for every time step and be accumulated to a partial $E_{comp,i} = dE_{comp,i} + E_{comp,i-1}$. If $E_{comp,i}$ becomes higher than E_f the particle will break.

The methodology described in this section is only applied if a particle is in simultaneous contact with more than one element. In the case of single contact between only two elements, nothing will prevent the separation of the elements after impact.

During a continuous contact, the damage (D) is not calculated. After the end of the contact between two particles (or between a particle and the geometry), if E_{comp} has not reached the value of E_f, the original methodology is applied, with the calculation of D and a new value of E_f.

III.3 Procedure for creation of the fragments distributions sets

The procedure, described as follows, explains how to create the families or options of fragments that can replace a particle after breakage. Those families are created randomly, however accounting for the equations that describe the fragmentation of real particles. In this case a normalizable breakage function was assumed, that is, that the level of fragmentation is independent of the original particle size. Nevertheless, the algorithm proposed can be easily modified if a non-normalizable breakage is necessary.

This procedure must be performed before the beginning of the simulation in DEM for the material to be simulated. The algorithm possesses the following features:

- Utilizes the incomplete beta function for the mathematical description of the appearance function, as discussed in section II.1.1.3;
- Follows a $\sqrt[4]{2}$ ratio for the relative fragment sizes. These sizes are a fraction of the original particle diameter;
- Uses a random number generator that follows the binomial distribution specified by the number of trials and the probability of success for each trial. Keeping in mind that DEM and particle replacement are discrete methods, this distribution was selected due to its also discrete nature, generating only integers;

- The number of trials of the binomial distribution is the desired number of families and the probability of success is the fraction of material generated in a size class, dictated by the appearance function.

The algorithm used in creation of the families used in this work was written in Matlab (Mathworks) and receives as input the parameters of the incomplete beta function that were fitted on the basis of experiments. The algorithm is repeated for each desired t_{10} as follows:

1) Calculate the various t_n values using the incomplete beta function;
2) For a desired number of size classes n_c, creates an array of fractional sizes $D_i = 2^{-i/4}$, with *i* from 1 to n_c. Is important to keep in mind that the selection, by the user, of a large value of n_c will result in a bigger number new particle after each replacement;
3) Interpolate the fraction smaller than D_i from the curve $\frac{1}{n} \times t_n$ and calculates the fraction w_i retained;
4) Generate randomly ten numbers for each size class D_i using ten as the number of trials and the probability of success in each trial is $M_i/10{D_i}^3$. This will create a first attempt of ten families. ${D_i}^3$ is a relative mass of fragments in relation the original particle mass;
5) Verify if the total relative mass of the ten families randomly created is similar to the equivalent theoretical mass expected by the appearance function equations, by a margin of 5%. If not, discard the ten families and create ten more;
6) Repeat steps 4 and 5 until the desired number of families is reached.

The reason for creation of a package of only ten families until the total desired number of families is reached is that some packages will have 5% less mass that it should and some will have 5% more mass. If the user creates, for instance, 100 families per t_{10}, on average the system should reproduce the appearance function results correctly.

It is important to keep in mind that the DEM breakage model is designed to simulate pilot or industrial scale process. In such processes hundreds to thousands of particle suffer breakage. In this way small variabilities between particles will be compensated by the statistics of the particle population.

IV. MODEL VERIFICATION

IV.1 Fracture energy for initial particles

The first logical step after the API implementation consists in examining if the primary particles are properly created with E_f following equations II.1 and II.2, with E_f as a function of material parameters and size. In this particular case, particle size is equivalent to its diameter. For this purpose, a simple simulation was created in which particles are generated and dropped onto a surface. As mentioned in the previous section, the API assigns fracture energy values to each particle during its first contact with any other element in the simulation. This is the reason for dropping the particles against a surface. Figure IV.1 shows a picture of the simulation with the particle colored by fracture energy value.

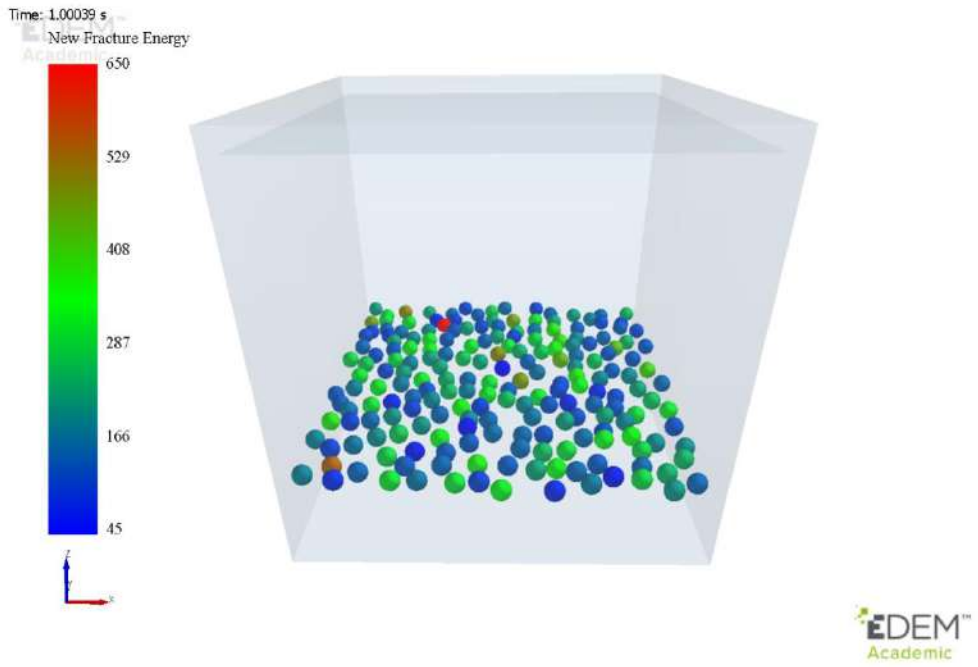

Figure IV.1 – Snapshot of the simulation used for checking the fracture energy distribution.

The simulation was conducted for two selected materials and three particle sizes. Table IV.1 presents the parameters for equations II.1 and II.2 for the materials simulated. After those initial simulations, the fracture energy values assigned to each of the particles were extracted and the results compared to those expected from the theoretical equations. Figure IV.2 presents this comparison for the two materials. Each point in Figure IV.2 represents one particle simulated. As can be seen, the ensemble of particles created by the API follows correctly the equations and parameters of the analytical model.

Table IV.1 – Selected material parameters used in API verification

	Material 1	Material 2
$E_{f\infty}$ (J/kg)	200	50
d_o (mm)	0.5	10.0
φ	0.90	0.50
σ_E	0.50	0.80

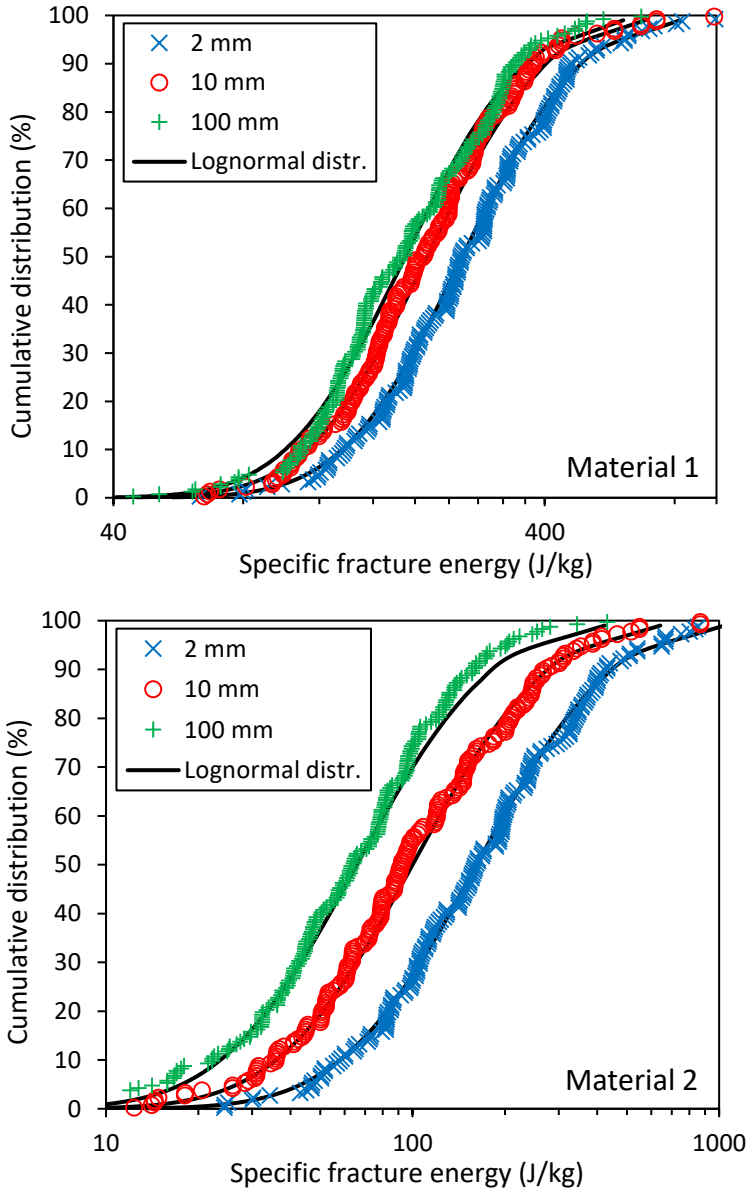

Figure IV.2 – Comparison of fracture energy distributions from the API (points) and equation II.1 (lines) for the two sets of parameters and different parent particle sizes.

It is important to point out that the API uses a random number generator to obtain the individual values for specific fracture energy and this generator is biased by the lognormal distribution. Due to this randomness of the assigned fracture energy values, the points in Figure IV.2 do not form a smooth curve. This feature can be considered an advantage of this procedure for simulation of real particle breakage since real brittle particles present similar variability.

IV.2 Simulation of damage accumulation

The second verification to be conducted was a simulation of a free fall experiment. In this experiment, real particles from a narrow size range are dropped, by free fall, against a steel surface from a given height. By the height and average mass of the particles the applied specific energy is estimated. The height is selected to be small enough not to cause breakage of all particles in a single drop. After a drop, the particle is collected and dropped again, with the tests being repeated until breakage occurs. Figure IV.3 presents a picture of the experimental set-up used by Cavalcanti (2015) for a system used in the laboratory to drop iron ore pellets from a height of 8.4 meters.

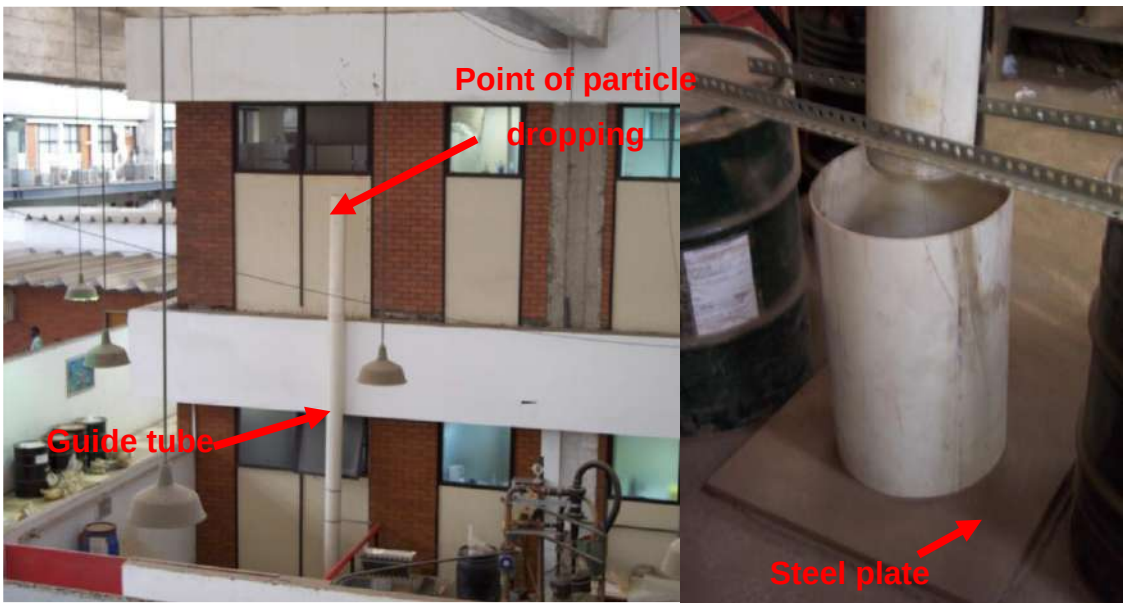

Figure IV.3 – Experimental set-up used for particle drop (Cavalcanti, 2015).

Assuming that the energy applied to the particles is equal in all impacts it is possible to measure how the fracture energy is reduced in each impact until it becomes smaller than

this applied energy, resulting in particle breakage. Although particles typically rebound after each drop, the applied energy resulting from the second or third impact in the same drop is assumed to be insufficient to cause a relevant change in the particle internal crack structure.

In order to test the ability of the API to simulate the fracture energy reduction in single impacts, the set-up described above was simulated in EDEM. Figure IV.4 shows a picture of section of the simulated domain where 80 particles were created and dropped from heights of 8.0 and 4.2 meters. The particles were positioned inside virtual guide tubes in order to avoid mixing of fragment particles after breakage. In these simulations, the particles are created at the selected height and dropped against a steel plate. After impact, the number of broken particles is counted and the fragments removed. For the second impact, the sign of the simulated gravity is inverted and the particles fall again, hitting a second steel plate at the top and so on.

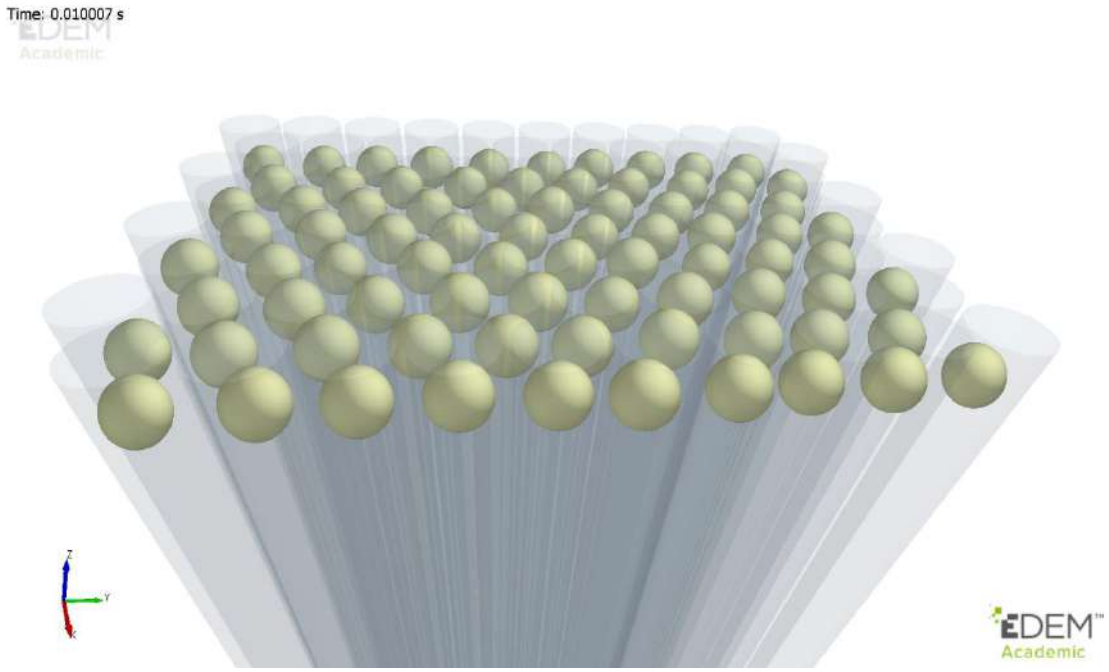

Figure IV.4 – Simulation to validate damage accumulation.

The material tested in this part of the work consisted of iron ore pellets and the breakage parameters were estimated by Cavalcanti (2015). The material and contact parameters required by the DEM contact model used were estimated by Barrios et al. (2013). Table IV.2 presents the parameters adopted in the simulations. The simulations were conducted at time steps of 5% of the Raleigh time. It was not observed, differences in

terms of the results as a function of the time step. However, it was observed that a time step bigger than 8% tend to cause instabilities during the replacement procedure due to high overlap between new particles.

In Figure IV.5 the results from the simulations (symbols) and those calculated from the theoretical equations II.7 and II.8. (lines) are compared. The values of impact energy used in the equations were obtained from the energy dissipated by the particle during the simulated impact. Again, the API was able to simulate the behavior of real particles with relatively good agreement with model results that were validated by experiments.

Considering that the simulated particles are idealized and their defined properties controlled by mathematical expressions, such as equations II.1-.8, it would be reasonable to expect that results from the simulation would exactly reproduce the results from direct application of the equations. For instance, in the case of Figure IV.5, one could expect the points to be in perfect agreement with the lines. However, due to the random nature of the properties assigned, e.g. fracture energy, the simulated particles end up presenting results that are more similar to those of real hard particles. Besides that, the use of the energy dissipated in the impact as the measure of severity of the collision also introduces a bias in the simulations.

Table IV.2 – Parameters applied the validation of damage accumulation

	Iron ore pellet
Size (mm)	10.6
$\boldsymbol{E_{f\infty}}$ (J/kg)	33.32
$\boldsymbol{d_o}$ (mm)	27.74
$\boldsymbol{\varphi}$	1.480
$\boldsymbol{\sigma_E}$	0.736
$\boldsymbol{\gamma}$	7.5
Coefficient of restitution	0.39

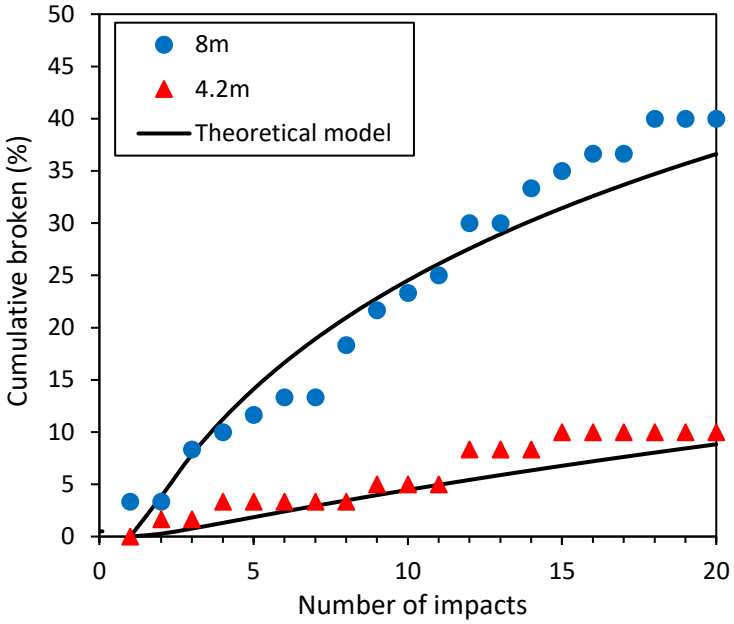

Figure IV.5 – Comparison of cumulative number of broken particles over repetitive impacts between API (points) and theoretical equations II.7 and II.8 (lines).

IV.3 Fragments generated after breakage

IV.3.1 Generalized breakage function and fragments distribution

The traditional application of this DEM breakage model requires experimental determination of many parameters related to breakage mechanisms. However, it is not uncommon for the DEM user to not have access to enough material samples, nor to the equipment or even the experimental experience to properly characterize the response of a given material to different breakage mechanisms. With that in mind, a complementary study was carried out on the basis of a large experimental database with the aim of seeking a set of parameters for the breakage function equations that could be used potentially as default in case not enough testing was conducted for a particular sample. As discussed in sections 2.2.3 and 3.2.3, the breakage function describes the distribution of fragment in size that are generated after particle breakage. In this work, the incomplete beta function was used for its mathematical formulation (Carvalho et al. 2015).

One of the most common experiments for the characterization of single-particle breakage function is the drop weight test (DWT). Over the years, *Laboratório de Tecnologia Mineral* from COPPE/UFRJ has accumulated a vast database of DWT results for many types of ores as well as rocks from different quarries. The size of the particles tested varied from 90 to 3.35 mm. This database was used for this study. Table IV.3

summarizes the different types of ores and rocks from this database and the number of samples characterized.

Table IV.3 – Ores characterized by drop weight test

Ore	Number of sets of data
Basalt	12
Bauxite	186
Limestone	199
Coal	72
Cassiterite ore	33
Cement clinker	159
Phosphate	45
Gneiss	73
Granulite	111
Copper ore	203
Niobium ore	27
Iron ore	279
Iron ore pellet	63
Quartz	12
Syenite	33

From the fragment size distribution curves resulting from DWT values of t_2, t_4, t_{10}, t_{25}, t_{50} and t_{75} were estimated. It was observed that nearly all the different types of ores characterized present a very similar t_{10} x t_n's relation. Figure IV.6 presents these relations for the studied samples. As can be seen, the different ore samples presented similar fragment distributions after breakage, which indicates that it is reasonable to adopt a single set of breakage function parameters for all ores. This is particularly useful in the case when proper sample for material characterization to be simulated is not available.

The parameters of the incomplete beta function were then fitted to the t_{10} x t_n's relations obtained. Each t_{10} x t_n set of points resulted in a pair of parameters (Z and W) presented in Table IV.4, whereas Figure IV.6 compares the fitted incomplete beta function curves to the experimental data.

It is important to point out that these results do not shows that all ores fragment in the same way when impacted by a given energy. The level of fragmentation, that describes how fine the fragments are in relation to the primary particle, is a function of applied energy and is modeled by the equation $t_{10} = A\left[1 - exp\left(-b'\, E_{cs}/E_{f50}\right)\right]$ presented in the literature review. The relation between different points of the fragment size distribution, described by the t_{10} x t_n curves is what can be assumed to be material independent, for the range of materials studied.

Table IV.4 – Fitted incomplete beta function parameters

	Z	W
t2	0.9592	5.7796
t4	1.1048	2.6186
t25	0.9809	0.5235
T50	0.9555	0.3389
T75	0.9338	0.2547

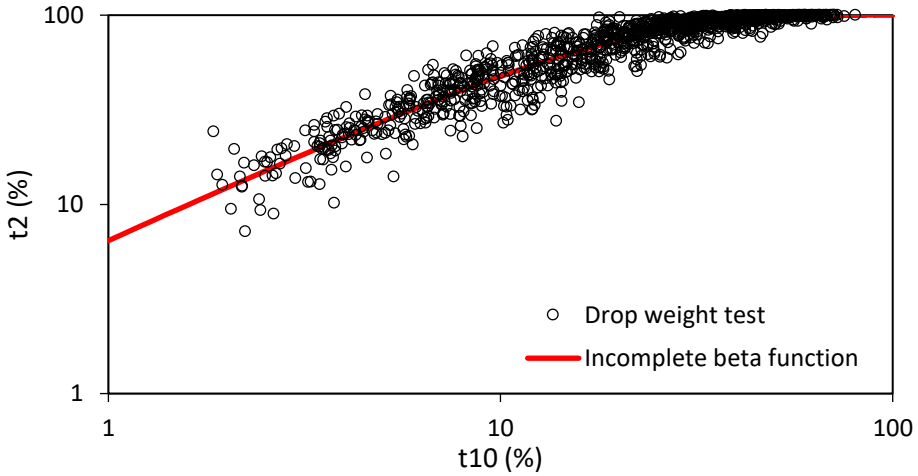

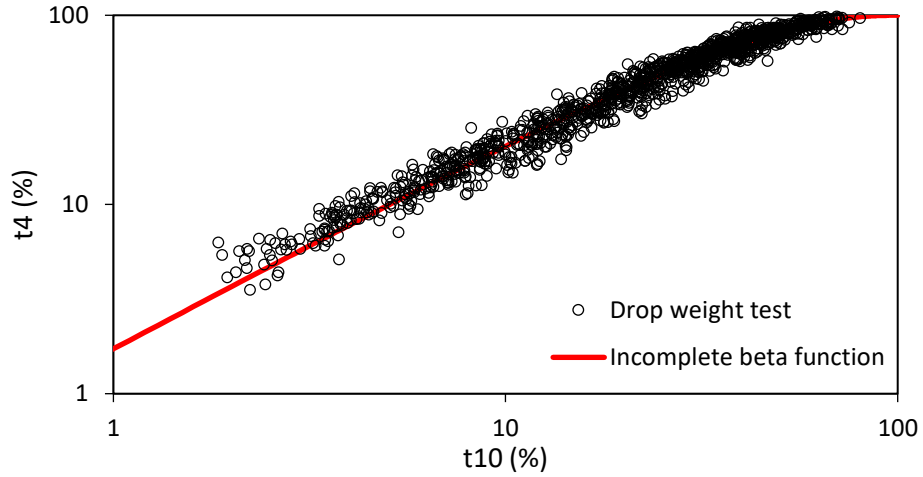
100
10
1
t4 (%)
1
10
100
t10 (%)
Drop weight test
Incomplete beta function

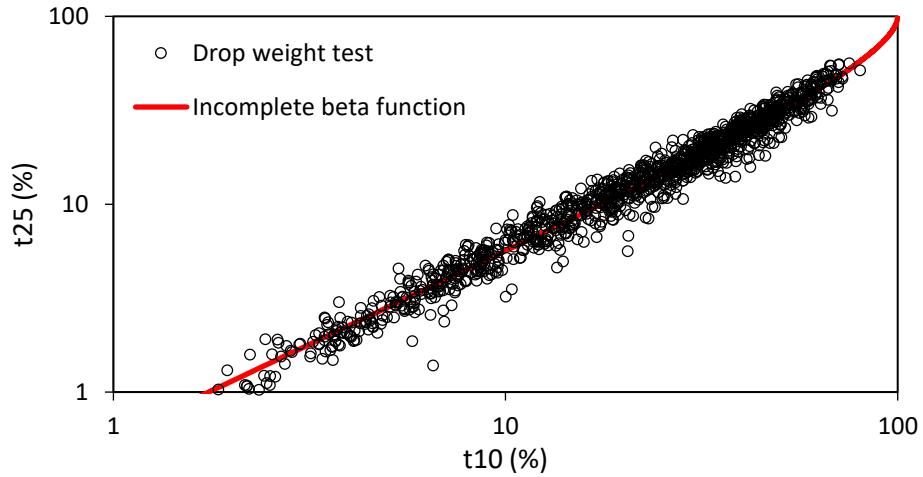
100
10
1
t25 (%)
1
10
100
t10 (%)
Drop weight test
Incomplete beta function

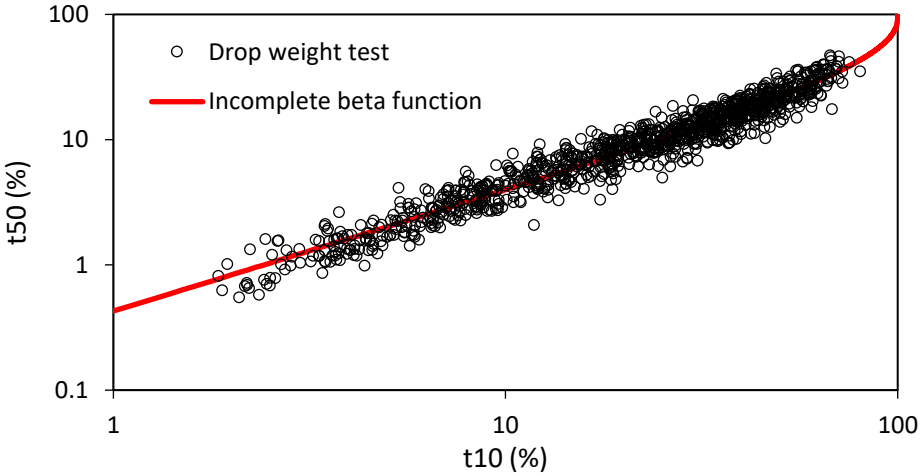
100
10
1
0.1
t50 (%)
1
10
100
t10 (%)
Drop weight test
Incomplete beta function

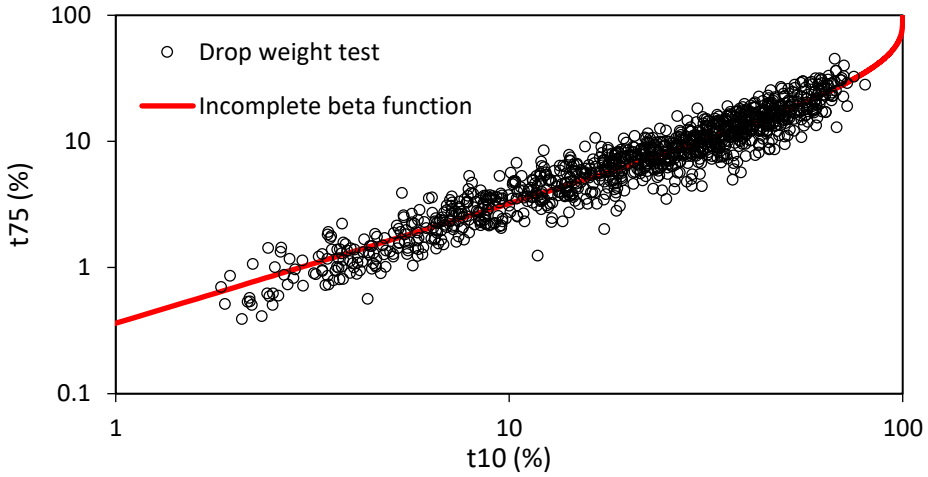

Figure IV.6 – Comparison between interpolated DWT results for all samples (points) with the fitted incomplete beta function (line).

Before simulating actual particle breakage, it was necessary to create the different sets of fragments sizes that would replace the broken particle, as discussed in section 3.2.3. Following the procedure presented in section 3.3, the set of fitted parameters presented in Table IV.4 was used the create a default matrix of fragments or distributions of daughter particles, with 100 options of fragments for each t_{10} value. In this way, every time a particle is considered broken in the simulation, the API will calculate t_{10} as a function of the energy dissipated and the particle fracture energy and randomly draw one family of fragments from the 100 available for the resulting value of t_{10}.

With the aim of demonstrating the validity of this approach for simulating the variability in individual particle fragmentation, Figure IV.7 presents how well a size distribution from breakage of single particles may be simulated as the number of broken particles increases for each value of t_{10}. In the figure, the black line presents the target size distribution curve directly calculated using the incomplete beta function with the parameters in Table IV.4. The figure also presents the total fragment size distribution for the breakage of one, five and ten particles of the same size, with each breakage resulting in a different combination of fragments, randomly selected.

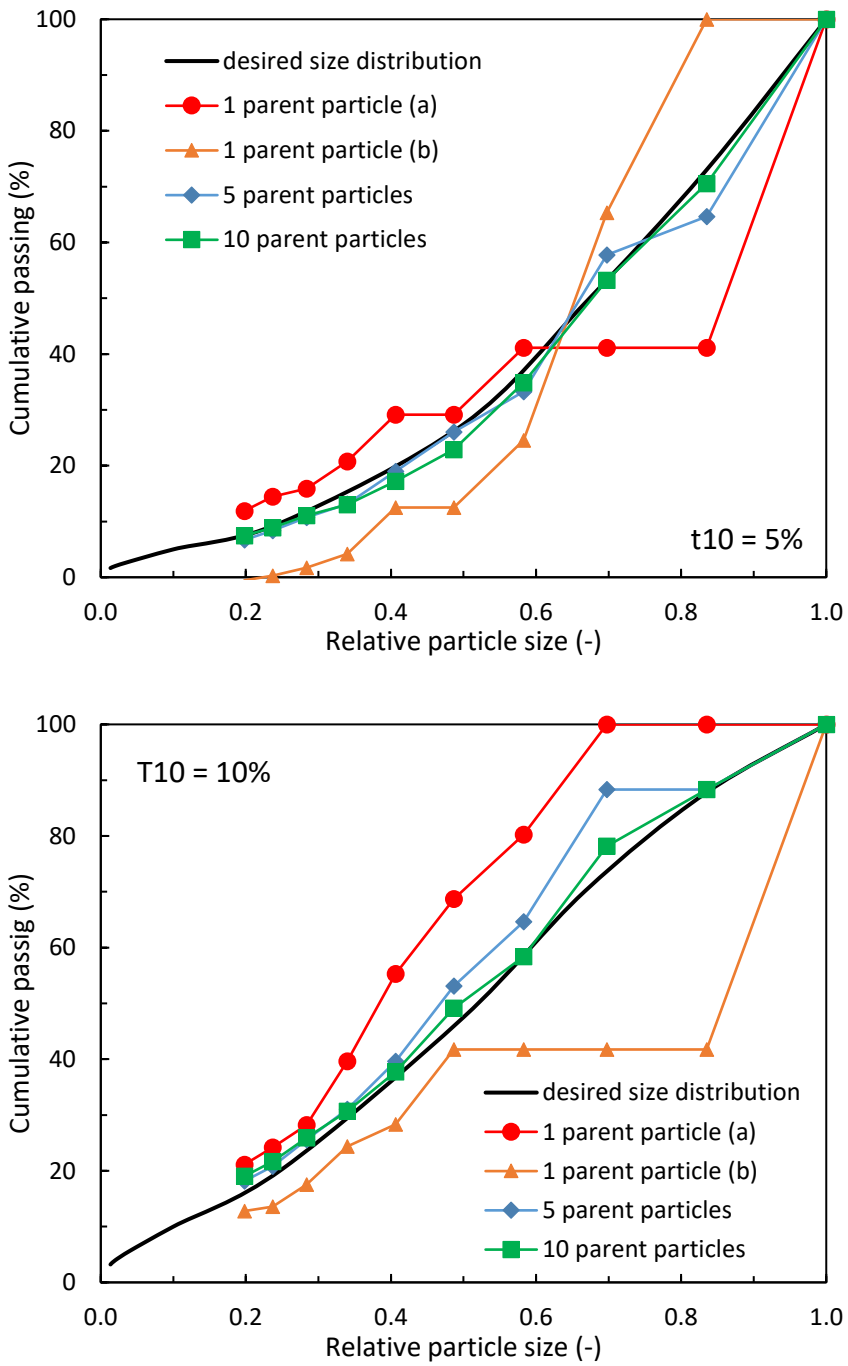

Figure IV.7 – Representation of theoretical fragments distribution with the families of fragments for different values of t_{10}.

In the case of breakage of a single particle, Figure IV.7 presents two (*a* and *b*) different options of fragments. As can be seen, in the case of just one broken particle, it is not possible to reach a distribution that resembles that for the desired curve. However, in the case of breakage of five particles, the resulting curve created by the total collection of fragments is already much closer to the desired curve. Finally, in the case of ten particles,

the fragment size distribution from the simulations approaches that from desired curve, obtained using the analytical model. Considering that the main objective of this DEM breakage model is the simulation of real industrial grinding process, where much more than 10 particles would break, the methodology of breaking each particle differently is capable of representing real results.

IV.3.2 Simulation of the drop weight tests

For verifying the particle replacement procedure and fragment size distribution the drop weight test (DWT) was simulated. The DWT consists in letting an impactor, usually made of steel, of known mass drop against the tested particle. The impactor considered for this work was a steel ball. During the test the ball falls under gravity to crush a single particle that is placed on a steel anvil. By changing the release height as well as the mass of the steel ball, a wide range of input energies can be produced. The test is repeated for a large number of individual particles, usually above 50, with an input energy that is high enough to ensure particle breakage in a single impact. For the simulation of DWT, a total of sixty particles are impacted simultaneously, as presented in Figure IV.8. The steel balls were created at a given height from the particles, that are sitting on a steel surface.

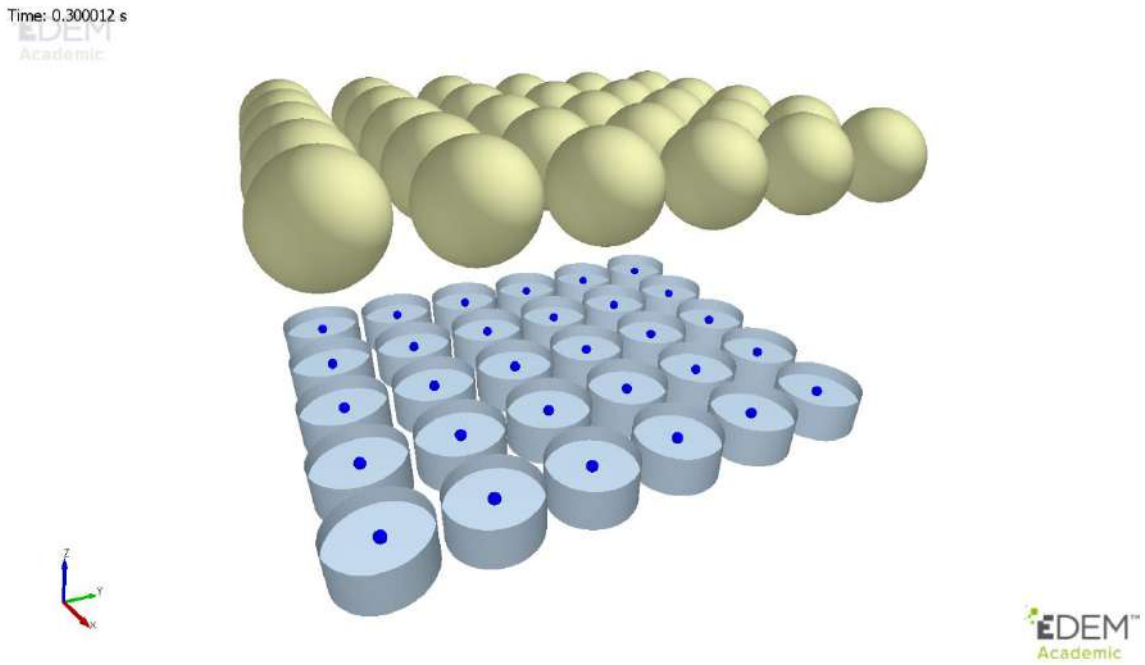

Figure IV.8 – Simulation of the drop weight test in EDEM. The small blue spheres are the tested particles.

In Figure IV.9 the replacement step of the API is presented, showing the particle before and after the impact. The figure is visualized from the bottom, in the direction of the falling ball. In the first time step after breakage determination by the API, the original particle is removed and the fragments created with geometrical centers inside the its volume. As explained in chapter three, the fragments are created having a considerable overlap. After replacement, the new particles can move freely with no difference from original particles.

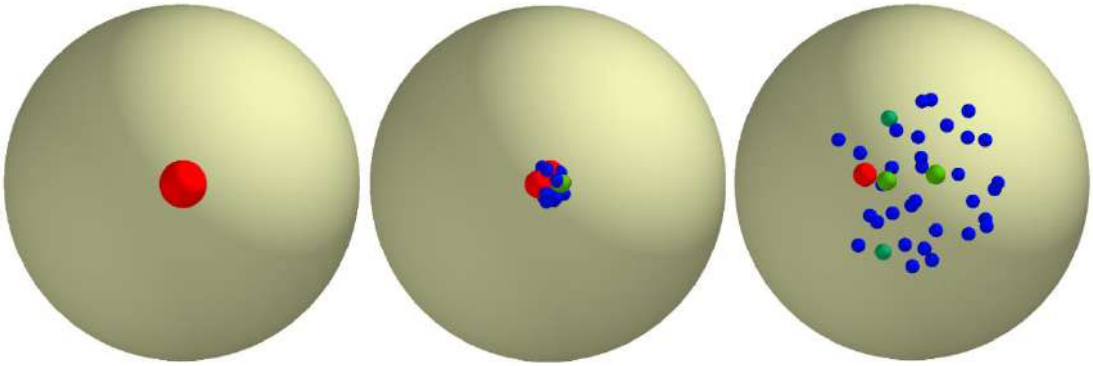

Figure IV.9 – Tested particle before impact (left), after first replacement (center) and after end of the impact (right). The particles are colored by diameter, with the original particle having 20.6 mm in size.

For the DWT simulation copper ore particles were considered, with sizes between 22.4 and 19.0 mm. Table IV.5 presents the parameters for theoretical equations used in these simulations. Those parameters were fitted on the basis of previous works at the *Laboratório de Tecnologia Mineral* (Carvalho & Tavares, 2013). The parameters for the breakage function and incomplete beta function used are presented in Table IV.4. The families or options of fragments, as discussed in sections 3.2.3 and 4.3.1, were created prior to the simulations following the procedure described previously. The selected time step was 1% of the Raleigh time. Different than the simulation in the previous section, in the DWT case, particles are compressed between two surfaces, impactor and base, what causes a confinement in the replacement region and entails more instabilities.

Three input energies were simulated and the results are presented in Figure IV.10. The figure also presents the results from the theoretical model. The impact energies were calculated according to equation IV.10 below, with E_{imp} in kWh/t. M_{ball} is the mass of the steel ball measured in kg, H_b is the height of fall in cm and m_{part} is the mass of the

impacted particles in g. For the sake of simplicity, the input energy was varied by artificially changing the steel ball mass, with the drop height kept constant.

$$E_{imp} = \frac{0.0272 \cdot M_{ball} \cdot H_b}{m_{part}} \quad \text{(IV.1)}$$

Table IV.5 – Parameters applied the validation of drop weight test simulations.

Parameters	Copper ore
$\boldsymbol{E_{f\infty}}$ (J/kg)	60.0
$\boldsymbol{d_o}$ (mm)	400
$\boldsymbol{\varphi}$	0.45
$\boldsymbol{\sigma_E}$	0.80
$\boldsymbol{\gamma}$	5.0
$\boldsymbol{A}$ (%)	67.7
$\boldsymbol{b'}$	0.029
Coefficient of restitution	0.39

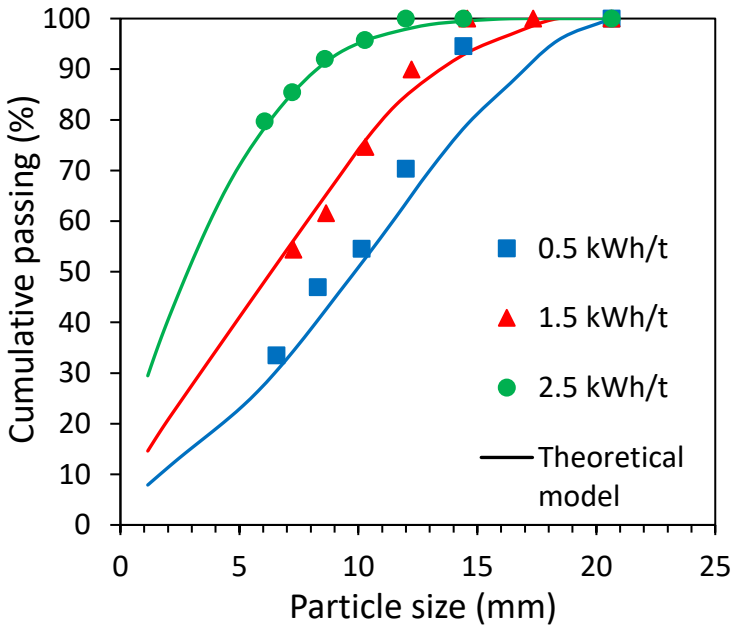

Figure IV.10 – Comparison of fragment size distributions for DWT, where points represent the simulated (API) and the lines are results of the theoretical equations. The material used was copper ore particles contained in size 22.4 - 19.0 mm.

The results presented for each specific impact energy represent the sum of all the fragments from the original sixty particles, presenting good correspondence with the theoretical equations predictions.

In order the keep the simulation time reasonable and sustain the stability of the simulation, sizes of fragments could only be created with a minimum value of 25% of the original particle diameter. It is important to consider that the smaller the new particle created, the larger the number of individual elements. Additionally, the larger the number of particles created in the confined volume of the mother particle, the higher are the repulsive forces and the number of contacts to be resolved by the software. This simplification requires ignoring the mass of fragments smaller than 25% of the original diameter, otherwise the size distribution of the fragments would not respect the prediction of the theoretical equations.

In order to conserve the mass of the original particle, without simulating the smaller fragments, the amount of mass that was missing after replacement, from the original particles, is added to the finest size allowed to be created. This option, however, creates an artificially large number of fragments in the finest size.

The lack of adoption of this simplification does not represent a large source of deviation from real results for low impact energies, such as in the case of input energies smaller than 0.5 kWh/t, that results in t_{10} values below 10% for most materials. However, for high input energies, above 1 kWh/t, the copper ore considered, for instance, this would present fragments with t_{10} of around 20%. Without this simplification, by applying high input energies, the simulation would lose more than 20% of the mass from each broken particle after replacement.

V. Conclusions

The selection of the particle replacement method for direct simulation of particle breakage in DEM presents some advantages in relation to other alternatives. This method presents smaller computational effort by only handling the fragments after breakage detection, in contrast with the bonded particle method that computes the fragments since the beginning of the simulation. Additionally, the modelling of particles as spheres facilitates the detection of contacts during simulation in relation to tetrahedral shapes. In the case of spheres, the particles center and radius are enough information to describe both contact and overlapping volume, while when a tetrahedral is used, the software needs to consider orientation and relative position of all vertices to resolve the contacts. Another advantage is direct definition of particle properties, such as the criterion for breakage and fragments size. With the exception of the technique proposed by Tavares et al. (2020), all other DEM breakage approach calibration of parameters related to breakage simulation. The methodology presented here allows direct use of material properties measured independently by standard tests procedures, without requiring calibration.

The breakage model presented here, based on the particle replacement method, allows selection, by the user, of particle properties using experimental data and without requiring calibration procedures. For instance, the breakage criteria and fragments size can be obtained by slow compression of single or bed of particles. The model also adds variability to the simulation respecting the statistics of real material properties. The breakage model additionally has flexibility to include, remove or change breakage mechanisms. As an example, the fragments sizes can be modelled as a single or multiple distribution options and, by that adding or removing variability in sizes. The user can also define the number of size classes fragments can occupy and create new particles as small as desired.

The breakage model proposed here was implemented in a API and included on a commercial DEM software. The results of the simulations show that the API simulates correctly the energy required for breakage of single particles. The API simulated with good agreement to experimental results weakening of particles over repetitive low energy impacts until breakage. On the case of high energy impacts, the API correctly determined breakage of particles and the replacement procedure simulated the fragmentation according to experimental results from drop weight tests. Those results indicate that this API would be a reliable tool for simulation grinding process, such as crushing. Crushers are particular good candidates for simulation since are traditionally operated in passage mode with very small residence times. In this way particles enter

the device, suffer breakage and leave the grinding zone, without many additional stressing events.

VI. Future works

In order to avoid an exponential increase in the number of particles simulated, the current version of the proposed methodology requires the selection of a minimum fragment size to be created after breakage. The original particles mass can be conserved, or not, depending on the user, by adding the mass of fine particles into the minimum size created. One way or another, the information about the size distribution of very fine particles is not maintained. One suggestion for future development is numerically preserving the information, during simulation, of the size distribution of particles smaller than the minimum size, possibly as mass by size matrix. At the end, this information could be accessed during post-processing.

One phenomenon that can be readily implemented to this technique is the generation of fine particles due to surface abrasion. During low energy impacts, particle might suffer only internal damage and not break. However, some small amount of fine particle is lost from the mother particle surface without meaningful loss in mass or size. Cavalcanti et al. (2019) proposed a methodology for estimation of the surface breakage by low energy impacts that can be directly implemented in DEM in a future update of the model.

VII. References

Austin, L.G. & Concha, F., 1994. Diseño y simulación de circuitos de molienda y clasificacion, Universidad Técnica Federico Santa María Ediciones.

Barrios, G.K.P., Carvalho, R.M., Kwade, A., Tavares, L.M., 2013. Contact parameter estimation for DEM simulation of iron ore pellet handling. Powder Technology, 248, pp.84–93.

Barrios, G.K.P., Carvalho, R.M. & Tavares, L.M., 2011. Modeling breakage of monodispersed particles in unconfined beds. Minerals Engineering, 24(3–4), pp.308–318.

Barrios, G.K.P. & Tavares, L.M., 2016. A preliminary model of high pressure roll grinding using the discrete element method and multi-body dynamics coupling. International Journal of Mineral Processing, 156, pp.32–42.

Barrios, G.K.P., Tavares, L.M. & Pérez-Prim, J., 2015. DEM Simulation of Bed Particle Compression Using the Particle Replacement Model. In Proceedings of the 14th European Symposium on Comminution and Classification. Gothenburg, pp. 59–63.

Baumgardt, S., Buss, B., May, P., Schubert, H., 1975. On the comparison of results in single grain crushing under different kinds of load. In Proceedings of the 11th International Mineral Processing Congress. Cagliari, p. 3.

Bbosa, L.S., Powell, M.S. & Cloete, T.J., 2006. An investigation of impact breakage of rocks using the split Hopkinson pressure bar. Journal of The South African Institute of Mining and Metallurgy, 106(4), pp.291–296.

Brouwers, H.J.H., 2006. Particle-size distribution and packing fraction of geometric random packings. Physical Review E, 74(3), p.31309.

Brown, R.L. & Richards, J.C., 1970. Principles of powder mechanics P. Press, ed., Edinburgh: Elsevier.

Carvalho, R.M., 2013. Mechanistic modelling of semi-autogenous grinding. Doctoral Thesis, Universidade Federal do Rio de Janeiro.

Carvalho, R.M. & Tavares, L.M., 2013. Predicting the effect of operating and design variables on breakage rates using the mechanistic ball mill model. Minerals Engineering, 43–44, pp.91–101.

Carvalho, R.M., Tavares, L.M. & Secchi, A.R., 2015. A new breakage function model and optimization procedure for mechanistic comminution models. In Proceedings of the 14th European Symposium on Comminution and Classification. Gothenburg, pp. 42–45.

Cavalcanti, P.P.S., 2015. Calibração e validação de modelo matemático de degradação de pelotas de minério de ferro durante manuseio e transporte. M.Sc. thesis, Universidade Federal do Rio de Janeiro.

Cavalcanti, P.P., Carvalho, R.M., Chagas, A.S., Silveira, M.W., Tavares, L.M., 2019. Surface breakage of fired iron ore pellets by impact. Powder Technology, 342, pp. 735-743.

Cho, N., Martin, C.D. & Sego, D.C., 2007. A clumped particle model for rock. International Journal of Rock Mechanics and Mining Sciences, 44(7), pp.997–1010.

Ciantia, M.O. Arroyo, M., Calvetti, F., Gens, A., 2015. An approach to enhance efficiency of DEM modelling of soils with crushable grains. Géotechnique, 65(2), pp.91–110.

Cleary, P.W., 2001. Recent advances in DEM modelling of tumbling mills. Minerals Engineering, 14(10), pp.1295–1319.

Cleary, P.W. & Sawley, M.L., 2002. DEM modelling of industrial granular flows: 3D case studies and the effect of particle shape on hopper discharge. Applied Mathematical Modelling, 26(2), pp.89–111.

Cleary, P.W. & Sinnott, M.D., 2015. Simulation of particle flows and breakage in crushers using DEM: Part 1 – Compression crushers. Minerals Engineering, 74(15), pp.178–197.

Cundall, P.A., 1988. Formulation of a three-dimensional distinct element model—Part I. A scheme to detect and represent contacts in a system composed of many polyhedral blocks. International Journal of Rock Mechanics and Mining Sciences & Geomechanics Abstracts, 25(3), pp.107–116.

Cundall, P.A. & Strack, O.D.L., 1979. A discrete numerical model for granular assemblies. Géotechnique, 29(1), pp.47–65.

Cunha, E.R., 2014. Modelagem mecanicista de britadores de impacto de eixo vertical, Doctoral thesis, Universidade Federal do Rio de Janeiro.

Cunha, E.R., Carvalho, R.M. & Tavares, L.M., 2013. Simulation of solids flow and energy transfer in a vertical shaft impact crusher using DEM. Minerals Engineering, 43–44, pp.85–90.

Curry, J.A., Ismay, M.J.L. & Jameson, G.J., 2014. Mine operating costs and the potential impacts of energy and grinding. Minerals Engineering, 56, pp.70–80.

Delaney, G.W., Morrison, R.D., Sinnott, M.D., Cummins, S., Cleary, P.W., 2015. DEM modelling of non-spherical particle breakage and flow in an industrial scale cone crusher. Minerals Engineering, 74, pp.112–122.

Delaney, G.W., Cleary, P.W., Sinnott, M.D., Morrison, R.D., 2010. Novel application of DEM to modelling comminution processes. IOP Conference Series: Materials Science and Engineering, 10.

DEM Solutions, 2013. EDEM 2.5 User Guide., pp.1–141.

Fandrich, R.G., Clout, J.M.F. & Bourgeois, F.S., 1998. The CSIRO Hopkinson Bar Facility for large diameter particle breakage. Minerals Engineering, 11(9), pp.861–869.

Groot, R.D. & Stoyanov, S.D., 2011. Close packing density and fracture strength of adsorbed polydisperse particle layers. Soft Matter, 7(10), pp.4750–4761.

Herbst, J.A., Potapov, A., Hambidge, G., Rademan, J., 2008. Modeling of diamond liberation and damage for Debswana kimberlitic ores. Minerals Engineering, 21(11), pp.766–769.

Herbst, J.A. & Potapov, A.V., 2004. Making a Discrete Grain Breakage model practical for comminution equipment performance simulation. Powder Technology, 143–144, pp.144–150.

Hertz, H., 1882. Über die Berührung fester elastischer Körper. Journal für die reine und angewandte Mathematik, 92, pp.156–171.

Jiménez-Herrera, N., Barrios, G.K.P., Tavares, L.M., 2018. Comparison of breakage models in DEM in simulating impact on particle beds. Advanced Powder Technology, 29, pp. 692-706.

Johansson, M., Quist, J., Evertsson, M., Hulthén, E., 2016. Cone crusher performance evaluation using DEM simulations and laboratory experiments for model validation. Minerals Engineering.

Johnson, K.L., 1985. Contact Mechanics, Cambridge University Press.

Khanal, M. & Morrison, R.D., 2008. Discrete element method study of abrasion. Minerals Engineering, 21(11), pp.751–760.

King, R.P., 2001. Modeling and Simulation of Mineral Processing Systems. In Modeling and Simulation of Mineral Processing Systems. Oxford: Butterworth-Heinemann, pp. v–vi.

King, R.P. & Bourgeois, F.S., 1993. Measurement of fracture energy during single-particle fracture. Minerals Engineering, 6(4), pp.353–367.

Langston, P.A., Al-Awamleh, M.A., Fraige, F.Y., Asmar, B.N., 2004. Distinct element modelling of non-spherical frictionless particle flow. Chemical Engineering Science, 59(2), pp.425–435.

Legendre, D. & Zevenhoven, R., 2014. Assessing the energy efficiency of a jaw crusher. Energy, 74(C), pp.119–130.

Li, H., McDowell, G.R. & Lowndes, I., 2014. Discrete element modelling of a rock cone crusher. Powder Technology, 263, pp.151–158.

Lichter, J., Lim, K., Potapov, A., Kaja, Dean, 2009. New developments in cone crusher performance optimization. Minerals Engineering, 22(7–8), pp.613–617.

Lim, W.L. & McDowell, G.R., 2005. Discrete element modelling of railway ballast. Granular Matter, 7(1), pp.19–29.

Majidi, B. et al., 2015. Packing density of irregular shape particles: DEM simulations applied to anode-grade coke aggregates. Advanced Powder Technology, 26(4), pp.1256–1262.

Marigo, M. & Stitt, E.H., 2015. Discrete Element Method (DEM) for Industrial Applications: Comments on Calibration and Validation for the Modelling of Cylindrical Pellets. KONA Powder and Particle Journal, 32(32), pp.236–252.

Mindlin, R.D. & Deresiewicz, H., 1953. Elastic spheres in contact under varying oblique forces. Journal of Applied Mechanics, 20, pp.327–344.

Mishra, B.K., 2003. A review of computer simulation of tumbling mills by the discrete element method: Part II—Practical applications. International Journal of Mineral Processing, 71(1–4), pp.73–93.

Mishra, B.K. & Rajamani, R.K., 1992. The discrete element method for the simulation of ball mills. Applied Mathematical Modelling, 16(April), pp.598–604.

Misra, A. & Cheung, J., 1999. Particle motion and energy distribution in tumbling ball mills. Powder Technology, 105(1–3), pp.222–227.

Napier-Munn, T.J. et al., 1996. Mineral comminution circuits: their operation and optimisation, Indooroopilly: Julius Kruttschnitt Mineral Research Centre, University of Queensland.

Narayanan, S.S. & Whiten, W.J., 1988. Determination of comminution characteristics from single-particle breakage tests and its application to ball-mill scale-up. Transactions of the Institute of Mining and Metallurgy, (97), pp.C115–C124.

Potapov, A.V. & Campbell, C.S., 1996. A three-dimensional simulation of brittle solid fracture. International Journal of Modern Physics C, 7(5), pp.717–729.

Potapov, A.V. & Campbell, C.S., 1994. Computer Simulation of impact-induced particle breakage. Powder Technology, (81), pp.207–216.

Potapov, A.V. & Campbell, C.S., 1997. Computer simulation of shear-induced particle attrition. Powder Technology, 94(2), pp.109–122.

Potapov, A.V. & Campbell, C.S., 2000. The breakage induced by a single grinding ball dropped onto a randomly packed particle bed. Powder Technology, 107(1–2), pp.108–117.

Potapov, A.V., Hopkins, M.A. & Campbell, C.S., 1995. A two-dimensional dynamic simulation of solid fracture part i: description of the model. International Journal of Modern Physics C, 6(3), pp.371–398.

Potyondy, D.O. & Cundall, P.A., 2004. A bonded-particle model for rock. International Journal of Rock Mechanics and Mining Sciences, 41(8), pp.1329–1364.

Potyondy, D.O., Cundall, P.A. & Lee, C.A., 1996. Modelling rock using bonded assemblies of circular particles. In 2nd North American Rock Mechanics Symposium, 19-21 June, Montreal, Quebec, Canada. pp. 1937–1944.

Powell, M.S., Govender, I. & McBride, A.T., 2008. Applying DEM outputs to the unified comminution model. Minerals Engineering, 21(11), pp.744–750.

Quist, J. & Evertsson, C.M., 2016. Cone crusher modelling and simulation using DEM. Minerals Engineering, 85, pp.92–105.

Silveira, M.A.C.W., 2012. Modelagem da degradação de pelotas de minério de ferro durante o manuseio e transporte. Universidade Federal do Rio de Janeiro.

Sinnott, M.D. & Cleary, P.W., 2015. Simulation of particle flows and breakage in crushers using DEM: Part 2 – Impact crushers. Minerals Engineering, 74(15), pp.163–177.

Spettl, A., Dosta, Maksym, Antonyuk, S., Heinrich, S., Schmidt, V., 2015. Statistical investigation of agglomerate breakage based on combined stochastic microstructure modeling and DEM simulations. Advanced Powder Technology, 26(3), pp.1021–1030.

Tavares, L.M., 2009. Analysis of particle fracture by repeated stressing as damage accumulation. Powder Technology, 190(3), pp.327–339.

Tavares, L.M., 2007. Chapter 1 Breakage of Single Particles: Quasi-Static. In Handbook of Powder Technology. pp. 3–68.

Tavares, L.M., 1999. Energy absorbed in breakage of single particles in drop weight testing. Minerals Engineering, 12(1), pp.43–50.

Tavares, L.M., 1997. Microscale Investigation of Particle Breakage Applied to the Study of Thermal and Mechanical Predamage. University of Utah.

Tavares, L.M., 2004. Optimum routes for particle breakage by impact. Powder Technology, 142(2–3), pp.81–91.

Tavares, L.M. & Carvalho, R.M., 2009. Modeling breakage rates of coarse particles in ball mills. Minerals Engineering, 22(7–8), pp.650–659.

Tavares, L.M. & Carvalho, R.M., 2010. A Mechanistic Model of Batch Grinding in Ball Mills. In XXV International Mineral Processing Congress. Brisbane, pp. 1287–1297.

Tavares, L.M. & Carvalho, R.M., 2012. Modeling ore degradation during handling using continuum damage mechanics. International Journal of Mineral Processing, 112–113, pp.1–6.

Tavares, L.M., André, F.P., Potapov, A., Maliska Jr., C., 2020. Adapting a breakage model to discrete elements using polyhedral particles. Powder Technology, 362, pp. 208-220.

Tavares, L.M. & King, R.P., 2002. Modeling of particle fracture by repeated impacts using continuum damage mechanics. Powder Technology, 123(2–3), pp.138–146.

Tavares, L.M. & King, R.P., 1998. Single-particle fracture under impact loading. International Journal of Mineral Processing, 54(1), pp.1–28.

Tavares, L.M. & Neves, P.B., 2008. Microstructure of quarry rocks and relationships to particle breakage and crushing. International Journal of Mineral Processing, 87(1–2), pp.28–41.

Unland, G. & Szczelina, P., 2004. Coarse crushing of brittle rocks by compression. International Journal of Mineral Processing, 74S, pp.S209–S217.

Weerasekara, N.S., Powell, M.S., Cleary, P.W., Tavares, L.M., Evertsson, M., Morrison, R.D., Quist, J., Carvalho, R.M., 2013. The contribution of DEM to the science of comminution. Powder Technology, 248, pp.3–4.

Whiten, W.J. & Narayanan, S.S., 1983. Breakage characteristics of ores for ball mill modelling. Proceedings of AusIMM, 286(31).

Yashima, S., Kanda, Y. & Sano, S., 1987. Relationships between particle size and fracture energy or impact velocity required to fracture as estimated from single particle crushing. Powder Technology, 51(3), pp.277–282.

Yashima, S., Morohashi, S. & Saito, F., 1979. Single Particle Crushing under Slow Rate of Loading. Science Reports of Research Institutes, 28(116).

Zhao, L. et al., 2016. Laboratory-scale validation of a DEM model of screening processes with circular vibration. Powder Technology, 303, pp.269–277.